# Depth-dependence of soil organic carbon additional storage capacity in different soil types by the 2050 target for carbon neutrality

~~Chirol,~~ Clémentine Chirol[1,2], ~~Séré,~~ Geoffroy Séré[1], ~~Redon,~~ Paul-Olivier Redon[3], ~~Chenu,~~ Claire Chenu[2], ~~Derrien,~~ Delphine Derrien[4,5]

[1]Université de Lorraine, INRAE, LSE, F-54000 Nancy, France
[2]INRAE, AgroParisTech, Ecologie fonctionnelle et écotoxicologie des agroécosystèmes, Palaiseau, France
[3]Andra, Direction Scientifique & Technologique, Centre de Meuse/Haute-Marne, 55290 Bure, France
[4]INRAE, UMR SAS 1069, L'Institut Agro, Rennes, France
[5]INRAE, Centre de Nancy, Biogéochimie des Ecosystèmes Forestiers, F-54280 Champenoux, France
~~[4]INRAE, Centre de Nancy, Biogéochimie des Ecosystèmes Forestiers, F-54280 Champenoux, France~~

*Correspondence to*: Clémentine Chirol (clementine.chirol@inrae.fr)

**Abstract.** Land planning projects aiming to ~~maximise~~ maximize soil organic carbon (SOC) stocks are increasing in number and scope, often in line with the objective to reach carbon neutrality by 2050. In response, a rising number of studies assess ~~SOC additional storage capacities~~where additional SOC could be stored over regional to global spatial scales. In order to provide realistic values transferrable beyond the scientific community, ~~targets for~~studies providing targets of SOC accrual ~~potential~~~~SOC storage capacity assessments~~ should consider the timescales ~~over which this capacity might be reached~~needed to reach ~~those targets~~them~~it~~, taking into consideration the effects of~~considering the effects of~~ C inputs, soil type and depth on soil C dynamics.

This research was conducted in a 320 km$^2$ territory in North-eastern France –where eight contrasted soil types have been identified, characterized and mapped thanks to a high density of fully-described soil profiles. Continuous profiles of SOC stocks were interpolated for each soil type and land use (cropland, grassland or forest). We defined potential targets for SOC accrual using percentile boundary lines, and used a linear model of depth-dependent C dynamics, to explore the C inputs necessary to reach those targets within 25 years. We also used values from the literature to model C input scenarios, and provided maps of~~Depth-dependent estimates of maximum SOC additional storage capacity using the Hassink equation and a data-driven approach were compared. We used a novel method that uses the data-driven approach to constrain C inputs in a simple model of depth-dependent C dynamics to simulate SOC accrual over 25 years, and mapped the~~ SOC stocks, maximum ~~additional storage~~SOC accrual ~~capacity~~ and realistic SOC accrual over 25 years.~~stock evolution.~~

SOC stocks and maximum SOC accrual~~dditional storage capacities~~ are highly heterogenous over the region of study. Median SOC stocks range from 78 - 333 tC ha$^{-1}$. ~~Data-driven maximum SOC additional storage capacities~~Maximum SOC accrual ~~potential~~ varies~~y~~ from 19 tC ha$^{-1}$ in forested Leptosols to 197 tC ha$^{-1}$ in grassland Gleysols. ~~Estimations of SOC maximum additional storage capacities based on the Hassink approach led to unrealistic vertical distributions of SOC stock, with~~

**Mis en forme :** Couleur de police : Texte 1
**Mis en forme :** Couleur de police : Texte 1
**Mis en forme :** Couleur de police : Texte 1
**Mis en forme :** Couleur de police : Texte 1
**Mis en forme :** Couleur de police : Texte 1
**Mis en forme :** Couleur de police : Texte 1
**Mis en forme :** Couleur de police : Texte 1
**Mis en forme :** Couleur de police : Texte 1

particular overestimation in the deeper layers.T But tTCrucially, the simulated realistic SOC accrual over 25 years in the whole region of study was five times lower than the maximum SOC additional storage capacity accrual (0.57 and 2.5 Mg C respectively). Further consideration of depth-dependent SOC dynamics in different soil types is therefore needed to provide targets of SOC storage over timescales relevant to public policies aiming to approach carbon neutrality by 2050.

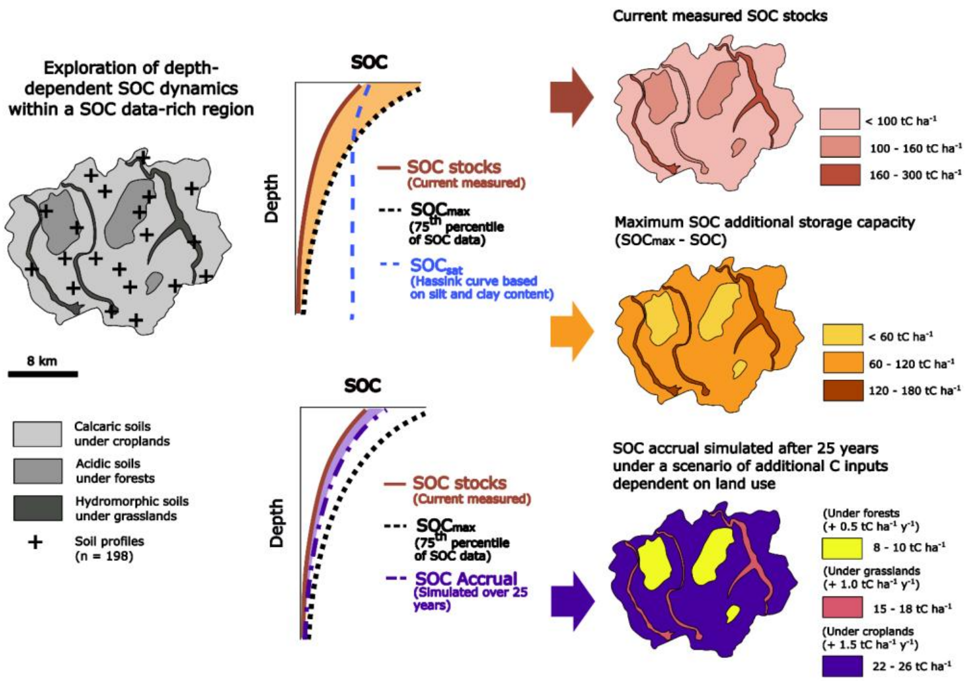


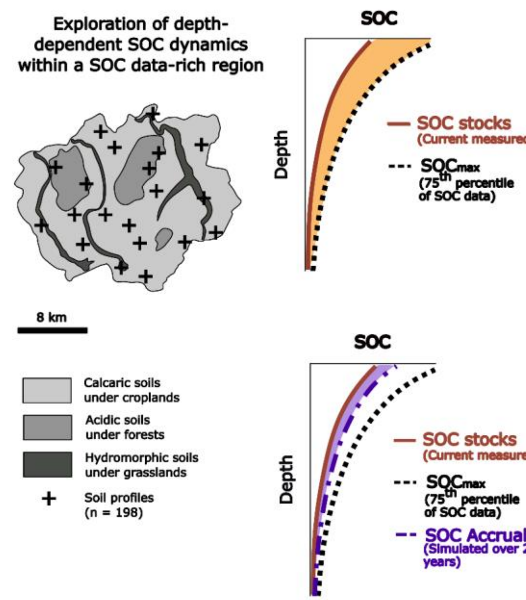

## 1 Introduction

Soils constitute a carbon reservoir that can help us mitigate for climate change, or conversely accelerate GHG emissions if not managed properly. Objectives for carbon neutrality by 2050 rely on an increase in soil organic carbon (SOC) via changes in land management practices over the coming decades, while preserving existing stocks (Minasny et al.et al., 2017). There is a rising demand for the scientific community to provide quantitative targets for SOC accrual for stakeholders at regional scales and over decadal timescales. However, soils are heterogenous and dynamic systems: soil carbon stocks are constantly being mineralized and renewed by new inputs. The spatial heterogeneity of soil carbon stocks and fluxes presents a challenge to soil carbon sequestration strategies. Certain soils may represent large stocks that need to be preserved, while others may have a greater capacity for ~~additional storage~~ SOC accrual. ~~We need to provide quantitative targets for SOC sequestration for stakeholders at regional scales and over decadal timescales.~~ Estimation of SOC stocks and SOC stock accrual potential should be performed over the whole soil profile because SOC below 20 cm can account for more than 50% of the total stock (Jobbágy & Jackson, 2000; De Vos ~~et al.~~ *et al.*, 2015). Impacts of management practices on SOC dynamics have been found to vary above and below 30 cm, so the consideration of the whole soil profile is ~~also~~ important to provide accurate recommendations to stakeholders (Tautges ~~et al.~~ *et al.*, 2019).

T~~hese t~~argets of SOC accrual are currently estimated using two distinct concepts. ~~:~~ ~~t~~The first is the fine fraction saturation approach, using ~~one uses~~ the clay and silt content as a proxy of the maximum carbon content that a given soil is theoretically able to stabilize in ~~in~~ association with mineral phases (Hassink 1997, Angers ~~et al.~~ *et al.*, 2011). ~~;~~ ~~t~~The other is ~~the maximal SOC accrual approach~~ based on the analysis of current ecosystems' functioning: this method seeks the highest observed SOC stock from a dataset taken in a given pedoclimatic context, and assumes this stock to be a realistic target under the management practices captured by the ~~is~~ dataset (Lal 2016, Chen ~~et al.~~ *et al.*, 2019~~a~~). In this study we will adapt this method to define depth-dependent targets as a continuous profile. approach will not be used due to our focus on the whole soil profile: at depth, SOC storage becomes limited by diminishing organic matter inputs, therefore carbon saturation in the fine fraction is unlikely to be a pertinent constraint on maximum SOC [illegible]

[illegible]

neutrality objective by 2050. Getting the kinetics of SOC accrual necessitates a model-driven approach and scenarios of C inputs to the soil (Barré ~~et al.~~ *et al.*, 2017). Mechanistic models of SOC dynamics such as Millenial (Abramoff ~~et al.~~ *et al.*, 2022) are one option to incorporate the effect of climate change and modifications in management practice, but necessitate a lot of input data, therefore simpler models remain valuable to explore (Derrien ~~et al.~~ *et al.*, 2023; ~~,~~ Schimel 2023). For some studies, simple linear models dependent on C inputs have proven to be sufficient to capture respiration patterns across different soils and SOC levels, even though temporal fluctuation in respiration fluxes were not properly represented (Fujita *et al.*, 2014). We will use a linear model that contains a fast cycling, ~~and~~ a slow cycling and an inert pool. Pool size and turnover have been calibrated by Balesdent *et al.* (2018) using a global database of C concentrations and 13C isotopes measured after a change in vegetation in multiple campaigns, principally over several decades. This calibration makes the Balesdent *et al.* (2018) parameters singularly robust to estimate C accrual over 25 years.

In addition to land use (Guo & Gifford, 2002), the physico-chemical properties of the soil play an important role on SOC accumulation and residence time (Kögel-Knabner *et al.*, 2021). Soil properties that affect SOC stabilization ~~notably~~ include the clay content and exchangeable cations (Rasmussen ~~et al.~~ *et al.*, 2018). High $Ca^{2+}$ concentrations in soils were found to intensify SOC accumulation either through increased occlusion within aggregates or through enhanced SOC association with minerals (Rowley ~~et al.~~ *et al.*, 2021). Low pH values also hinder microbial activity and organic matter degradation, leading to an increased residence time of SOC in the soil (Malik ~~et al.~~ *et al.*, 2018). The parameters from Balesdent *et al.* (2018) in the model [illegible] SOC dynamics are impacted by climate change, both directly through the effects of soil temperature and moisture on C decomposition rates, and indirectly through modifications in soil properties (Luo *et al.*, 2017).

Once targets of SOC accrual have been set for a given timescale, the next step to facilitate communication with stakeholders [illegible]

The main objective of this paper is to ~~-~~ estimate and map realistic targets for SOC accrual within decadal timescales, accounting for soil type and depth. To that end, we will explore the effect of land use and soil type on whole-profile SOC stocks and decadal dynamics. We focus on a region of study where dense data collection has taken place and where land use change has seen very little variation for 200 years ~~over timescales relevant to stakeholders (25 years), and how SOC accrual over decadal timescales might differ from the maximum SOC additional storage capacity as estimated by current methods~~. ~~We have chosen to use a model that has been calibrated over the soil profile by Balesdent *et al.* (2018) using C isotopes tracing over timescales of several decades to several centuries. The originality of our approach resides in the use of data-driven estimates of maximum SOC additional storage capacity combined with the depth-resolved model by Balesdent *et al.* (2018) to obtain the input scenarios required to reach the maximum SOC stocks of the studied area at the steady state. The~~We use a combination of pre-existing methods (interpolation of continuous SOC profiles, estimation of~~percentile approach to obtain~~ theoretical ~~a continuous profile of~~ maximum SOC stocks based on observed values~~s~~, application of a simple model of C dynamics robust at decadal timescales, mapping of the simulated SOC accrual ~~scenario~~ after 25 years) ~~is~~ as an innovative way of generating realistic results that are transferrable beyond the scientific community. We will explore two scenarios of SOC accrual: one where we apply annual C inputs necessary to reach the theoretical maximum SOC stock within 25 years, and one where we apply realistic C input values found in the literature. We will also explore scenarios with different rates of temperature increase by 2050 following climate change scenarios RCP4.5 and RCP8.5.

**~~Ecrire ici scenarios de realistic inputs et elevation des temperatures~~**

**2.1 Study site and data acquisition**

The Perennial Observatory of the Environment (OPE in French) is monitoring since 2007 a 320 km$^2$ area located in the North-Eastern part of France (in Meuse and Haute Marne counties). This observatory operated by the Radioactive Waste Management Agency (ANDRA) aims to follow the environmental impacts of a planned deep underground nuclear waste storage facility. In the framework of the monitoring program, various environmental data including soil characterization and mapping have been collected.

The OPE study area is dominated by agricultural and forest lands: 55% of the region is occupied by agricultural lands managed by conventional agriculture practices; 29% is occupied by forests dominated by deciduous trees (oak, charm, beech); 14% is occupied by grassland, and less than 2% by urban areas. A land occupation map from 1830 shows that limited modifications in land use have taken place over the past 200 years (Dupouey *et al.*, 2008). The region's continental climate is softened by

**Mis en forme :** Couleur de police : Texte 1

**Mis en forme :** Police :Non Gras, Couleur de police : Texte 1

**Mis en forme :** Couleur de police : Texte 1

**Mis en forme :** Police :Non Gras, Couleur de police : Texte 1

**Mis en forme :** Couleur de police : Texte 1

**Mis en forme :** Couleur de police : Texte 1

some oceanic influences. According to data collected by the OPE weather stations from 2009 to 2019, the mean annual temperature is 10.4 °C (+/- 6.2 °C between summer and winter), annual cumulated rainfall is 983 mm (+/- 113) and ETP = 661 mm (+/- 79).

This study uses a total of 198 soil profiles (932 ~~data points~~samples) to estimate SOC stocks and ~~additional storage capacity~~maximum SOC accrual. 86 of these soil profiles were collected within the region of study between 1995 and 2019, and were used along with a 1/50,000 pedological map (Party ~~*et al.*~~*et al.* / Sol Conseil 2019) to classify the soils into eight dominant soil types and define the physico-chemical characteristics of each of their horizons, such as pH, $CaCO_3$, texture and rock fragment content (Table 1~~See measurement protocols in Appendix Table 1~~). The eight identified soil types can be broadly divided based on the geological parent materials and the geomorphology of the region (Figure 1). On the plateaus, preserved detritic Cretaceous layers from the Valanginian stage with high concentrations of silt and sand lead to the formation of Eutric and Dystric Cambisols, with locally Podzosols reaching deeper than 2 m. On the hillslopes and in the valleys, the parent materials are Tithonian limestones and Kimmeridgian marls and limestones, leading to the formation of Calcaric to Hypereutric Cambisols with high rock fragment contents in the deeper horizons. Soils on the hillslopes, referred to as Rendzic Leptosols and Hypereutric Epileptic Cambisols, are more superficial and have higher rock fragment contents. Stagnosols and Gleysols can be found at the bottom of the valleys and over the Kimmeridgian marls and limestones: they are deep, clay-rich and hydromorphic soils; the former is waterlogged for part of the year while the latter is waterlogged all year round. In the north-east of the study area, clay-rich and $CaCO_3$-bearing materials from a tunnel excavation in 1841-1846 form local pockets of Technosols, which were not considered in this study due to their limited spatial extent. Land use information was derived from the 1/100,000 CORINE Land Cover 2018 at a resolution of 25 ha.

The data from the 86 soil profiles contain SOC content data in the different soil horizons (253 ~~data points~~samples), but only 48 bulk density measurements using the cylinder method. In order to provide additional SOC content and bulk density data as a function of depth, 112 additional profiles corresponding to these eight soil types were collected from soil databases in the six surrounding administrative geographical units (counties). The soil profiles were collected by the RMQS (French Soil Quality Monitoring Network) and Renecofor (French Permanent Plot Network for the Monitoring of Forest Ecosystems). In each collected sample, organic carbon content (g $kg^{-1}$) is measured in the fine fraction (< 2 mm) by dry combustion after removal of the inorganic carbon with acid. Since this study only considers mineral soil, the litter layer was excluded from the forest profiles. Bulk density values are measured using the cylinder method in 552 out of the 932 samples, and are otherwise estimated from a pedotransfer function from Beutler ~~*et al.*~~*et al.* (2017) based on clay and total organic content values as follows:

$$BD = [1.6179 - 0.0180 * (Clay + 1)^{0.46} - 0.0398 * SOC^{0.55}]^{-1.33} \quad (1)$$

where BD is the bulk density (kg $m^{-3}$), Clay is the clay content (g $kg^{-1}$), and SOC is the total organic carbon content (g $kg^{-1}$). The pertinence of this pedotransfer function to estimate bulk density in our region of study has been validated with the 48 samples from the region of study where bulk density measurements were available with a mean square error value of 0.70. Other pedotransfer functions from the literature (Saxton & Rawls, 2006; Akpa *et al.*, 2016; Shiri *et al.*, 2017) were also tested but gave mean square error values of 3.13, 6.81 and 353.35 respectively.

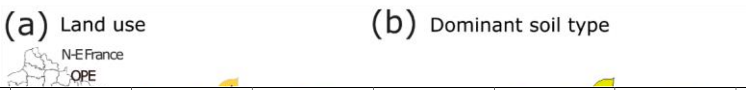


| **Soil Type** | **Horizon** | **Depth (cm)** | **Horizon Thickness (cm)** | **Clay (g kg$^{-1}$)** | **pH** | **Rock fragments (%)** | **CaCO$_3$ (g kg$^{-1}$)** |
|---|---|---|---|---|---|---|---|
| **Calcaric Rendzic Leptosols** | 1 | 35 (9) | 16 (5) | 478 (68) | 7.8 (0.9) | 3 (15) | 58 (118) |
| | 2 | | 19 (6) | 392 (123) | 8.3 (0.4) | 35 (30) | 414 (186) |
| **Calcaric Cambisol** | 1 | 60 (17) | 14 (6) | 462 (110) | 7.8 (0.9) | 8 (15) | 13 (136) |
| | 2 | | 21 (11) | 394 (87) | 8.2 (0.4) | 35 (23) | 465 (250) |
| | 3 | | 25 (11) | 328 (110) | 8.3 (0.3) | 70 (20) | 389 (246) |
| **Hypereutric epileptic Cambisol** | 1 | 43 (11) | 22 (7) | 489 (73) | 7.8 (0.8) | 0 | 0 |
| | 2 | | 21 (5) | 523 (86) | 6.9 (1.1) | 60 (31) | 0 |
| **Hypereutric Cambisol** | 1 | 84 (61) | 20 (6) | 409 (125) | 6.9 (1.0) | 2 (13) | 0 |
| | 2 | | 30 (14) | 522 (147) | 7.5 (0.7) | 3 (28) | 0 |
| | 3 | | 33 (45) | 733 (119) | 7.8 (0.4) | 50 (26) | 2 (5) |
| **Eutric Cambisol** | 1 | 85 (30) | 18 (6) | 278 (107) | 5.6 (0.8) | 0 | 0 |
| | 2 | | 27 (10) | 484 (164) | 6.2 (1.0) | 0 | 0 |
| | 3 | | 40 (28) | 595 (207) | 7.5 (1.5) | 5 (36) | 2 (17) |
| **Dystric Cambisol** | 1 | 168 (33) | 15 (5) | 40 (1) | 4.0 (0.2) | 0 | 0 |
| | 2 | | 18 (3) | 27 (6) | 4.3 (0.2) | 0 | 0 |
| | 3 | | 10 (0) | 40 (8) | 4.3 (0.2) | 0 | 0 |
| | 4 | | 48 (3) | 75 (9) | 4.7 (0.1) | 0 | 0 |
| | 5 | | 78 (23) | 95 (44) | 4.6 (0.1) | 0 | 0 |
| **Stagnosol** | 1 | 115 (30) | 28 (5) | 490 (182) | 7.8 (1.0) | 0 | 2 (196) |
| | 2 | | 40 (11) | 353 (131) | 8.2 (1.4) | 0 | 98 (244) |
| | 3 | | 47 (11) | 346 (111) | 8.4 (1.2) | 1 (15) | 576 (236) |
| **Gleysol** | 1 | 140 (41) | 23 (7) | 453 (88) | 7.8 (0.4) | 0 | 103 (105) |
| | 2 | | 46 (12) | 386 (62) | 8.2 (0.3) | 0 | 143 (189) |
| | 3 | | 72 (36) | 350 (75) | 8.2 (0.3) | 0 | 290 (288) |

**from 86 whole soil profiles sampled between 1995 and 2019 within the region of study. Standard deviations are given in brackets. See measurement protocols in Appendix A.**



**Mis en forme :** Police :Gras
**Tableau mis en forme**
**Mis en forme :** Police :Gras
**Mis en forme :** Police :Gras
**Mis en forme :** Police :Gras
**Mis en forme :** Police :Gras
**Mis en forme :** Police :Gras
**Mis en forme :** Police :Gras
**Mis en forme :** Police :Gras
**Mis en forme :** Police :Gras

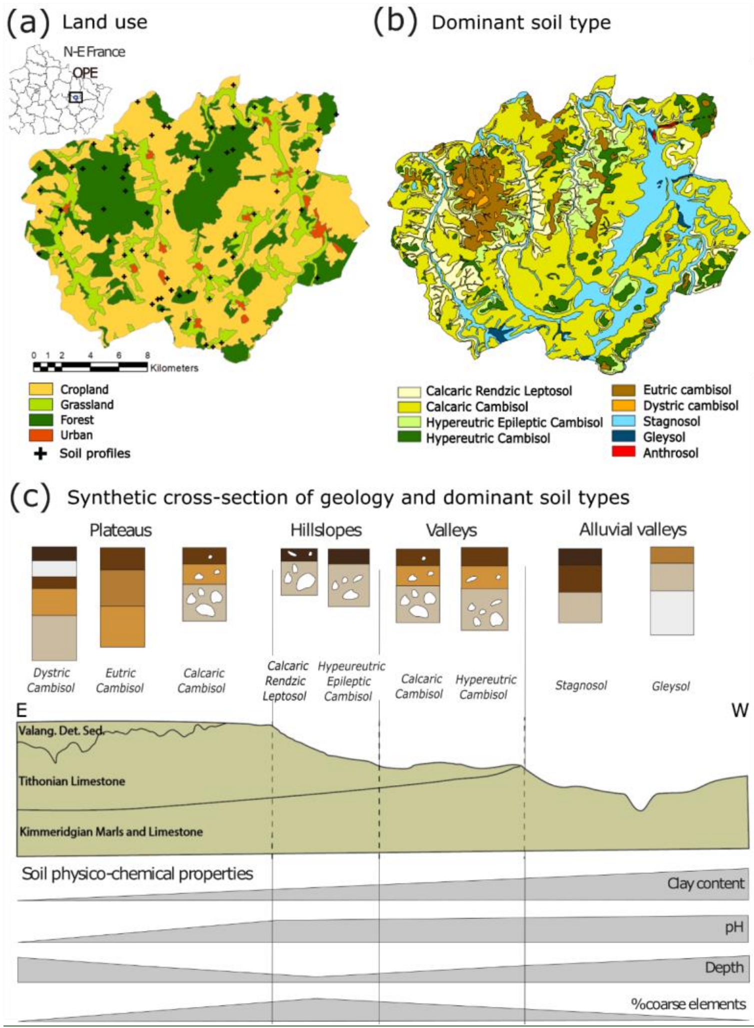


**Figure 1: Land uses, soil types and geomorphological context of the study region. (a) Land use (Source: Corine Land Cover 2018). (b) Map of dominant soil types (Source: Party ~~et al.~~*et al.*, 2019). (c) Synthetic cross-section of the geology, topography and dominant soil types in the region of study.**

### 2.2 Estimation of ~~current~~ initial and maximum SOC stocks

#### 2.2.1 ~~Current~~ Initial SOC stocks

Soil organic carbon stocks per surface unit are calculated as follows (Chen ~~et al.~~*et al.*, 2019~~a~~):

$$\mathrm{SOCstock} = \frac{p * \mathrm{SOC} * \mathrm{BD} * (100 - \%\ \mathrm{Rock\ fragments})}{1000} \quad \mathbf{(2)}$$

where $SOC_{stock}$ is the total SOC stock (kg $m^{-2}$), p is the soil ~~actual~~ thickness (m)~~ of topsoil or subsoil~~, SOC the soil organic carbon content (g $kg^{-1}$), BD the bulk density (kg $m^{-3}$ = g $dm^{-3}$) and % Rock fragments the percentage of elements > 2 mm (%). This methodology assumes that the fraction > 2 mm does not contain organic carbon, which has been disputed by Harrison ~~et al.~~*et al.* (2011) in cases where the rock fragments are abundant and display signs of porosity and weathering.

The median soil organic carbon content (SOC in g $kg^{-1}$) as a function of depth for each soil type and land use was calculated using the typical SOC content profile established by Mathieu ~~et al.~~*et al.* (2015) and Jreich (2018) on the basis of three descriptors: $\Omega_1$ the SOC content of the soil type at maximal depth, $\Omega_2$ the SOC content at the surface, and $\Omega_3$ the depth at half maximum of the SOC content:

$$\mathrm{SOC}\,(s,z) = \Omega 1(s) + (\Omega 2(s) - \Omega 1(s)) * e^{-(z/\Omega 3(s))} \quad \mathbf{(3)}$$

where *s* is the soil type, *z* the depth.

This method was used to interpolate SOC content data from national and regional datasets, acquired per horizon, in order to obtain the continuous distribution of SOC stock over the whole soil profile for each soil type and land use considered. A least square method for non-linear curve-fitting (Matlab function lsqcurvefit) was then applied to adjust the $\Omega_{1\text{-}3}$ parameters (Appendix ~~Table 2~~B).

Continuous vertical profiles of median bulk density were then obtained for each soil type using a logarithmic fit. The horizon thickness and percentage of rock fragments correspond to the median of the values per horizon per soil types in the 86 profiles within the OPE zone. This gave us a continuous profile of median SOC stocks as a function of depth, corresponding to the initial SOC stock profile. The dataset was collected between 1995 and 2019, but since land use has not changed since 1830, the soil profiles ~~can be~~were assumed to be at steady state, and to represent the initial SOC stocks before the implementation of C input modelling scenarios. The median SOC stock ~~is~~ was then calculated at each 1 cm interval along the whole profile based on the median bulk density curve, the median SOC curve and the percentage of rock fragments.

#### 2.2.2 Theoretical m~~M~~aximum SOC stocks and maximum SOC accrual

~~We call maximum SOC stocks the highest SOC stocks that a given soil type is estimated to be able to contain.~~ The theoretical maximum SOC stocks in this study are theoretical targets based on the upper values of the SOC data observed within the region. These targets represent the SOC stock that a given soil type can reach under the land management strategies represented in the region of study. The theoretical maximum SOC stock is therefore region-dependent as it is not solely driven by the intrinsic textural properties of the soil, but also by climate and the ecosystem plant productivity as they influence soil biology and chemistry along the soil profile. The maximum SOC ~~additional storage capacity~~accrual corresponds to the difference between the theoretical maximum SOC stock and [illegible]

The regression fit method applied using equation 3 from Jreich (2018) worked iteratively by first ~~find~~computing the 50th percentile boundary line (median profile corresponding to the initial SOC stocks) and removing all data points inferior to that line. The process was then repeated for the 75th percentile, then the 88.5th, and finally the 94th. The choice in percentile value strongly affects the estimation of maximum SOC stocks (Chen ~~et al.~~*et al.*, 2019~~a~~). In our case, since the number of SOC data points per soil type ranges from 29 (Hypereutric Epileptic Cambisol) to 268 (Stagnosol), the 75th boundary line is calculated based on 14 to 134 data points, the 88.5th percentile based on 7 to 67 data points, and the 94th percentile based on 3 to 34 data points. We chose the 75th boundary line ~~as our~~to defin~~ition~~e the theoretical maximum SOC stocks. ~~T~~We also calculated the 88th percentile boundary [illegible]

each soil type at 90% confidence interval (Chen ~~et al.~~*et al.* 2019~~a~~). W~~In this method, w~~e generated random subsets of input parameters SOC, BD, percentage of rock fragments and depth values within the standard deviation of each soil type, and repeated the procedure 1000 times to obtain 1000 estimates of the mean and percentiles values of the carbon stocks.

### 2.3 Simulation of SOC accrual at different timescales

[illegible] approach is illustrated in Figure 2, with further details of model functioning and equations in Appendix C.1. The profiles of initial SOC stocks were first discretized into 10 cm layers. In each layer, we applied a three-pool model with a fast cycling, a slow cycling pool and an inert pool, where the dynamic pools are ruled by exponential kinetics. SOC stocks do not saturate and are linearly dependent on C inputs for a given situation. Pools relative size and turnover were calibrated by Balesdent *et al.* (2018) using a global database of change in stable carbon (C3/C4) signatures measured over multiple campaigns, over decadal timescales, for ~~55~~112 grassland, forest and cropland sites. The C3/C4 approach is typically efficient to follow carbon dynamics over timescales ranging from one to one thousand years, especially compared to the $^{14}C$ method, which covers timescales of several thousand years (Verma *et al.*, 2017). We corrected the model parameters calibrated at the global scale in Balesdent *et al.* (2018) to account for local conditions of temperature, humidity, pH, clay content and $CaCO_3$ content as recommended by Rasmussen *et al.* (2018). This was done using the equations from the AMG model (Andriulo *et al.*, 1999; Saffih-Hdadi & Mary, 2008; Clivot *et al.* 2017; Levavasseur *et al.*, 2020). of depth derived from the corrected mineralization factors in the fast and slow pools can be found in Appendix ~~Table 3~~D.

**Mis en forme :** Couleur de police : Texte 1
**Mis en forme :** Couleur de police : Texte 1, Exposant
**Mis en forme :** Police :Non Gras, Couleur de police : Texte 1
**Mis en forme :** Couleur de police : Texte 1
**Mis en forme :** Couleur de police : Texte 1, Exposant
**Mis en forme :** Couleur de police : Texte 1
**Mis en forme :** Police :Non Gras, Couleur de police : Texte 1
**Mis en forme :** Couleur de police : Texte 1
**Mis en forme :** Couleur de police : Texte 1, Exposant
**Mis en forme :** Couleur de police : Texte 1
**Mis en forme :** Police :Non Gras, Couleur de police : Texte 1
**Mis en forme :** Couleur de police : Bleu foncé

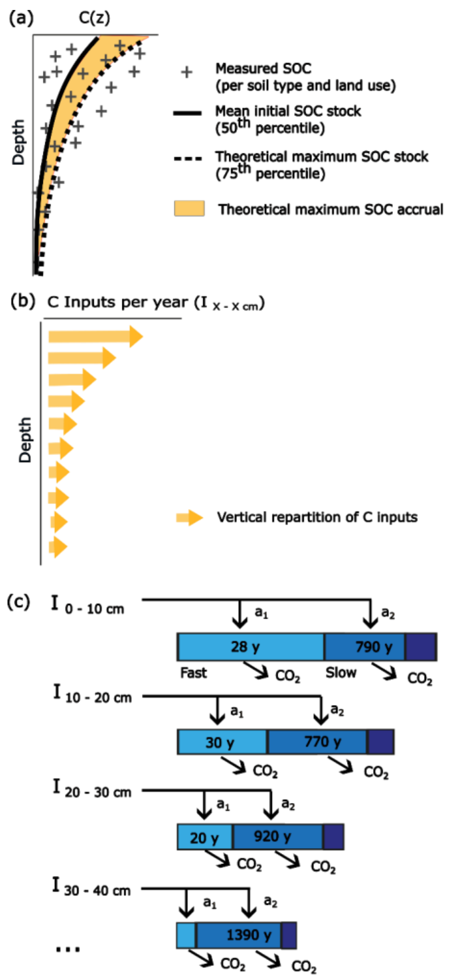


**Figure 2: Summary of our approach: (a) estimation of initial and theoretical maximum SOC stocks from the measured data; (b) estimation of vertical repartition of C inputs for the different scenarios considered, obtained by matrix inversion; (c) Functioning of the depth-dependent three-pool model (fast-cycling pool, slow-cycling pool, inert pool). a = allocation factor; MRT = Mean Residence Time (in years), y = years. MRT values vary with depth as per Balesdent *et al.* (2018) and are corrected for temperature, humidity, pH, texture and CaCO3; values displayed correspond to the mean MRT values per pool and depth section (see Methods for details and Appendix D for MRT values for each soil type and depth). The initial C inputs and maximum C inputs are provided in Appendix E.**

- [illegible] stocks in each soil type and land use, obtained by matrix inversion (Mao *et al.*, 2019): there is no SOC accrual in this case; **expliquer que c'est obtenu par inversion matricielle et référer au papier de Mao**
- *gain in after implementation of practices promoting C sequestration Scenario 2 (extreme input regime)* corresponds to the annual C inputs necessary to reach the theoretical maximum SOC stocks within 25 years, obtained through iterative optimization of the model; **Expliquer aussi comment c'est obtenu**
- *Scenario 3 (realistic increased input regime)* defines C inputs values higher than in scenario 1 that are compatible with the ranges of gain in C inputs after implementation of practices promoting C sequestration found in the literature: +0.5 tC ha$^{-1}$ y$^{-1}$ in forests, +1.0 tC ha$^{-1}$ y$^{-1}$ in grasslands, and +1.5 tC ha$^{-1}$ y$^{-1}$ in croplands.

For scenario 3, we sought values of typical current plant inputs and of realistic increased inputs from the literature or from existing data within the region of study. Typical current C inputs in forests range within 1.6 - 2.8 tC ha$^{-1}$ y$^{-1}$ according to measurements carried out in the Renecofor network in the region of study, assuming 50% mineralisation of above ground input in the forest floor. Changes in harvest practices towards non-export of harvest residues after thinning could provide additional inputs in the range of 0.5 – 2 tC ha$^{-1}$ y$^{-1}$ (total realistic input range: 1.6 – 4.8 tC ha$^{-1}$ y$^{-1}$). In grasslands, annual inputs to the soil range within 1.18 – 5.2 tC ha$^{-1}$ y$^{-1}$ according to studies from Australia and Western Europe (methods used: RothC inverse modelling, allometric equations using yield data, expert opinion) (Martin *et al.*, 2021). In croplands, annual inputs to the soil range within 1.8 – 6.8 tC ha$^{-1}$ y$^{-1}$ according to studies conducted worldwide (methods used: direct measurements, RothC inverse modelling, allometric equations using yield data, expert opinion) (Martin *et al.*, 2021).

Finally, we tested the effect of projected rises in temperature on the simulated SOC accrual by modifying the mineralization correction factor linked to temperature in the AMG model (see EquationAppendix Equation C1). The temperature was increased linearly to projected annual temperatures in metropolitan France in 2050the region of study according to the scenarios RCP4.5 (+1.0°C) and RCP8.5 (+1.0°C and +1.3 °C) according to model simulations by the Meteo France ALADIN63_CNRM-CM5 model within an 8 km radius area around Bure (55087), comparing the year intervals 2046-2055 and 2009-2019 (Drias, données Météo-France, CERFACS, IPSLfrom the mean temperatures of 1991-2020 respectively based on Soubeyroux *et al.*, 2020). This corresponds to an increase in mean annual temperatures from 10.4 °C to 11.4°C (RCP4.5) or 11.9°C (RCP8.5) over 25 years at all depths. The 1.0 °C increase in temperature in the region of study under scenario RCP4.5 was corroborated by model simulations of mean annual temperatures by the Meteo France ALADIN63_CNRM-CM5 model within an 8 km radius area around Bure (55087), comparing the year intervals 2046-2055 and 2009-2019 (Drias, données Météo-France, CERFACS, IPSL). RCP8.5 amounts to an extreme scenario in terms of increased mineralization rates, since in addition to using the most pessimistic RCP scenario, our model assumes that rises in temperature propagate instantly at depth and that humidity conditions remain at the present levels. We tested the sensitivity of SOC accrual to the two temperature scenarios in the different soil types and land covers.

**Mis en forme :** Police :Italique, Couleur de police : Texte 1

**Mis en forme :** Police :Italique, Couleur de police : Texte 1

**Mis en forme :** Paragraphe de liste, Avec puces + Niveau : 1 + Alignement : 1,9 cm + Retrait : 2,54 cm

**Mis en forme :** Couleur de police : Texte 1

**Mis en forme :** Couleur de police : Texte 1

**Mis en forme :** Police :Italique, Couleur de police : Texte 1

**Mis en forme :** Police :Non Gras, Italique, Couleur de police : Texte 1

**Mis en forme :** Police :Italique, Couleur de police : Texte 1

**Mis en forme :** Police :Non Gras, Italique, Couleur de police : Texte 1

**Mis en forme :** Couleur de police : Texte 1

**Mis en forme :** Police :Non Gras, Couleur de police : Texte 1

**Mis en forme :** Couleur de police : Texte 1


The study site was divided into zones characterized by their land use (cropland, grassland, forest) and by their dominant soil type. Mapping zZones were derived from the intersection of the CORINE Land Cover map and of the pedological soil map. Values of SOC stocks, maximum SOC accrual, and simulated accrual after 25 years were then associated to each mapping zone.

Mapping results are by necessity a simplification of the real distribution of soils properties and SOC contents. The soil units represented in Figure 1b shows [illegible] mapping zone contains several soil types that cannot be explicitly delimited on the map at this spatial resolution. Therefore, each point within a given zone has a probability of belonging to one of several soil types (e.g.: 70% chance of being a Eutric Cambisol, 30% chance of being a Stagnosol). The total SOC stock for thisa zone shouldis then be obtained by the weighted mean of the SOC stocks (e.g. 70 % of the SOC stock for Eutric Cambisols and 30 % of the SOC stock for Stagnosols). The standard deviation of the total SOC stock should likewise be obtained by the weighted standard deviations of the SOC stocks. The local uncertainty corresponds to expected local variations in the zone if the different soil types have contrasted SOC stocks. We visualized this local uncertainty by mapping the contrasts in SOC stocks within each zone in Appendix F.

## 3 Results

### 3.1 SOC stock and maximum additional storage capacitySOC accrual as a function of depth, land use and soil type

#### 3.1.1 Vertical repartition of SOC stocks

Current SOC stocks over the whole profile range from 78 to 333 tC $ha^{-1}$ (Table 32), of which 59 to 156 tC $ha^{-1}$ are in the topsoil (0 - 30 cm). The lowest SOC stocks are found in the shallower soil types (Calcaric Rendzic Leptosol and Hypereutric Epileptic Cambisol). Current SOC stocks are twice to three times higher in hydromorphic soils (Stagnosols and Gleysols) compared to non-hydromorphic soils.

SOC content and stocks decrease with depth, with sharp decreases in the SOC stock profiles corresponding to a change in the percentage of rock fragments between two horizons (Figure 3a-c). On average, excluding the shallower soil types (Calcaric Rendzic Leptosol and Hypereutric Epileptic Cambisol), the proportion of the SOC stock situated in the first 30 cm is 53 % in croplands, 67 % in grasslands and 71 % in forests (Appendix G). The soils in croplands are therefore depleted in SOC in the topsoil compared to forests and grasslands (Figure 3a). The difference in SOC stocks between land uses diminishes in the deeper horizons.

**percentile of our regional dataset, and SOC stock after 25 years under a realistic scenario of C inputs, for each soil type and land use. Realistic range of annual C inputs to the soil is 1.8 – 6.8 tC/ha/y for croplands (Martin *et al.*, 2020), 1.18 – 5.2 tC/ha/y for grasslands (Martin *et al.*, 2020), and 1.6 – 4.8 tC/ha/y for forests according to measurements made in the region of study.**

| Depth (cm) | | Initial SOC stock (90% confidence interval in brackets) (tC ha$^{-1}$) | Theoretical maximum SOC stock (75$^{th}$ percentile) (tC ha$^{-1}$) | Scenario 1: Initial input regime (tC ha$^{-1}$ y$^{-1}$) | Scenario 2: Extreme input regime (tC ha$^{-1}$ y$^{-1}$) | Scenario 3: Realistic increased input regime (tC ha$^{-1}$ y$^{-1}$) | SOC stock after 25 years under realistic increased input regime (tC ha$^{-1}$) |
|---|---|---|---|---|---|---|---|
| Calcaric rendzic leptosol | C | 78 *(48-115)* | 167 | 1.3 | 7.0 | 2.8 | 102 |
| | G | 101 *(84-138)* | | 1.9 | 6.0 | 2.9 | 118 |
| | F | 149 *(97-183)* | | 2.7 | 3.8 | 3.2 | 157 |
| Calcaric cambisol | C | 100 *(58-133)* | 191 | 1.8 | 7.9 | 3.3 | 123 |
| | G | 134 *(66-183)* | | 2.7 | 6.5 | 3.7 | 150 |
| | F | 148 *(104-184)* | | 2.8 | 5.7 | 3.3 | 156 |
| Hypereutric epileptic cambisol | C | 92 *(49-129)* | 129 | 1.5 | 3.8 | 3 | 117 |
| | F | 106 *(76-121)* | | 2.0 | 3.4 | 2.5 | 115 |
| Hypereutric cambisol | C | 103 *(62-137)* | 228 | 1.4 | 9.5 | 2.9 | 127 |
| | G | 167 *(125-255)* | | 2.5 | 6.4 | 3.5 | 183 |
| | F | 160 *(92-204)* | | 2.3 | 6.7 | 2.8 | 168 |
| Eutric cambisol | C | 102 *(59-144)* | 194 | 1.0 | 6.4 | 2.5 | 128 |
| | G | 90 *(66-115)* | | 1.2 | 7.4 | 2.2 | 107 |
| | F | 157 *(71-190)* | | 2.0 | 4.2 | 2.5 | 166 |
| Dystric cambisol | F | 120 *(76-198)* | 169 | 1.0 | 3.7 | 1.5 | 129 |
| Stagnosol | C | 166 *(101-237)* | 285 | 1.5 | 9.2 | 3 | 189 |
| | G | 161 *(108-279)* | | 1.9 | 9.8 | 2.9 | 177 |
| | F | 172 *(121-249)* | | 2.3 | 9.4 | 2.8 | 181 |
| Gleysol | C | 279 *(154-417)* | 476 | 2.8 | 17.3 | 4.3 | 301 |
| | G | 333 *(252-466)* | | 4.6 | 14.9 | 5.1 | 349 |

~~**Table 2: Soil organic carbon stocks, maximum stocks corresponding to the 75th percentile of the datasets under all land uses, and maximum SOC additional storage capacity estimated from the data-driven approach for the different land uses and soil types**~~

**Mis en forme :** Retrait : Gauche : 0,2 cm, Droite : 0,2 cm, Interligne : simple

**Mis en forme :** Retrait : Gauche : 0,2 cm, Droite : 0,2 cm, Interligne : simple

**Tableau mis en forme**

**Mis en forme :** Retrait : Gauche : 0,2 cm, Droite : 0,2 cm, Interligne : simple

**Mis en forme :** Retrait : Gauche : 0,2 cm, Droite : 0,2 cm, Interligne : simple

**Mis en forme :** Retrait : Gauche : 0,2 cm, Droite : 0,2 cm, Interligne : simple

**Mis en forme :** Retrait : Gauche : 0,2 cm, Droite : 0,2 cm, Interligne : simple

**Mis en forme :** Retrait : Gauche : 0,2 cm, Droite : 0,2 cm, Interligne : simple

**Figure 3: (a) Median (50th percentile of the dataset for each land use) and theoretical maximum (75th percentile of the dataset) fitted depth profiles of SOC content in each soil type~~ and each land use~~. The Jreich parameters (2018) used to plot the SOC content profiles are given in Appendix B~~Table 2~~. (b) ~~Estimation of maximum SOC content as a function of depth by the Hassink equation corrected with proportions of POM and MAOM from the literature (dashed blue line) and by the data-driven approach using a 75th percentile curve of the dataset (black solid line). (c)~~ Current SOC stocks under croplands and maximum SOC ~~additional storage capacity~~accrual to reach the theoretical maximum SOC stocks of each soil type.**

### 3.1.2 Theoretical M~~M~~aximum SOC stocks and maximum ~~additional storage capacity~~SOC accrual

The theoretical maximum SOC content ~~estimated by the data-driven approach~~ decreases with depth under all soil types, from 50-100 g kg$^{-1}$ near the surface to under 25 g kg$^{-1}$ at the bottom of the soil profiles (Figure 3a~~b-c~~). ~~By contrast, the decrease in maximum SOC content with depth as estimated by the Hassink equation is less prominent. Maximum total SOC contents stay~~

at around 35 - 46 g kg$^{-1}$ throughout all soil profiles (32 - 40 g kg$^{-1}$ under 30 cm), except for the Dystric Cambisol where the average value is 11 g kg$^{-1}$ (Figure 3b). The theoretical maximum SOC stocks as estimated by the data-driven approach range from 129 tC ha$^{-1}$ in the Hypereutric Epileptic Cambisol to 476 tC ha$^{-1}$ in the Gleysols.

The maximum SOC additional storage capacityaccrual found by the data-driven approach varies from 19 tC ha$^{-1}$ for shallow, rocky forest soils to 197 tC ha$^{-1}$ for agricultural Gleysols (Table 2), considering the a conversion of cropland into grassland or forest. Using percentile 88th instead of 75th increases our estimation of the maximum SOC stocks by about 16% (9 - 27% depending on soil type), without changing the hierarchy of maximum SOC stocks across the eight soil types.

### 3.2 Exploring kinetics of simulated SOC accrual

Employing the Hassink equation was considered to underestimate the maximum SOC content near the surface and to overestimate maximum SOC content in the deeper horizons, for reasons that will be detailed further in the Discussion section. The maximum SOC content profiles obtained by the data-driven approach were therefore selected for the exploration of SOC kinetics.

The stationary initial stationary C inputs obtained by model matrix inversion obtained by model inversion range are, depending on soil type, d from between 1.0 – 2.8 tC ha$^{-1}$ y$^{-1}$ for croplands, 1.2 – 4.6 tC ha$^{-1}$ y$^{-1}$ for grasslands and 1.0 – 2.8 tC ha$^{-1}$ y$^{-1}$ for forests (Table 2). By contrast, the extreme input regime needed to reach the theoretical maximum SOC stocks within 25 years ranges between 3.8 - 17.3 tC ha$^{-1}$ y$^{-1}$ for croplands, 6.0-14.9 tC ha$^{-1}$ y$^{-1}$ for grasslands and 3.4-9.4 tC ha$^{-1}$ y$^{-1}$ for forests. 1.0 - 4.6 tC ha$^{-1}$ y$^{-1}$, and the maximum C inputs from 1.4 - 6.0 tC ha$^{-1}$ y$^{-1}$ (Appendix Table 4). The realistic increased input regime chosen based on the literature is 2.5 – 4.3 tC ha$^{-1}$ y$^{-1}$ for croplands, 2.2 – 5.1 tC ha$^{-1}$ y$^{-1}$ for grasslands and 1.5 – 3.3 tC ha$^{-1}$ y$^{-1}$ for forests.

Under the chosen scenario of C inputs dependent on land use (+1.5 tC ha$^{-1}$ y$^{-1}$ under cropland, +1.0 tC ha$^{-1}$ y$^{-1}$ under grassland, +0.5 tC ha$^{-1}$ y$^{-1}$ under forest), realistic increased input regime, and when rising temperatures are not considered, the SOC accrual after 25 years ranges from 22-26 tC ha$^{-1}$ under cropland, 15-18 tC ha$^{-1}$ under grassland, to 8-10 tC ha$^{-1}$ under forest (Figure 4, Appendix Table 6H). Kinetics of SOC accrual are dependent on the time since the beginin of the adoption ofimplementation of the practice increasing C inputs to soil. The yearly accrual rates averaged over the first few decades is range betweentherefore 0.88-1.04 tC ha$^{-1}$ y$^{-1}$ under croplands, 0.6-0.72 tC ha$^{-1}$ y$^{-1}$ under grassland and 0.32-0.4 tC ha$^{-1}$ y$^{-1}$ under forest. The accrual rates then decrease over decadal and centennial timescales as the SOC stocks stabilise stabilize asymptotically towards the new steady state, as per the model equations. SOC accrual at the new steady state is highest under Dystric Cambisol owing to the effect of the low pH on the mineralization rates as implemented in the model. Modelled SOC accrual after 25 years decreases with depth under all soil types and land uses (Figure 5).

By contrast, reaching the maximum SOC stocks estimated by the 88$^{th}$ percentile required additional C inputs of about 3.4 tC ha$^{-1}$ y$^{-1}$ across all land uses. This was not considered realistic, as will be justified in the discussion section.

accrual simulated at constant temperature (10% under cropland, 20% under grassland and 30% under forest on average). The SOC accrual after 25 years under this scenario ranges from 16-24 tC ha$^{-1}$ under cropland, 10-16 tC ha$^{-1}$ under grassland, to 5-8 tC ha$^{-1}$ under forest (Appendix Table 6H).

Incorporating thee more extreme RCP8.5 scenario of 1.3 °C increase in temperature over 25 years attenuates SOC accrual by 10 to 50%, and shows a stronger impact of soil type and especially land cover on the mineralization rates (Appendix Table

**Mis en forme :** Couleur de police : Rouge foncé

~~6~~H). SOC accrual is attenuated by 10-20% in cropland soils, 10-40% in grassland soils, and 40-50% in most forest soils except Dystric Cambisols (20%).

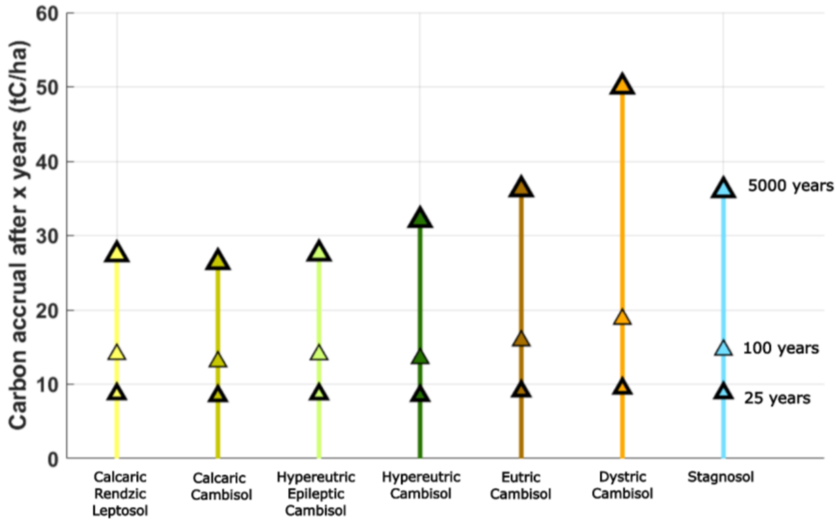


**Figure 4: Model results of SOC accrual after 25, 100 and 5000 years under forests for a scenario of +0.5 tC ha$^{-1}$ y$^{-1}$ compared to the ~~stationary~~ initial C inputs, temperature remaining constant.**

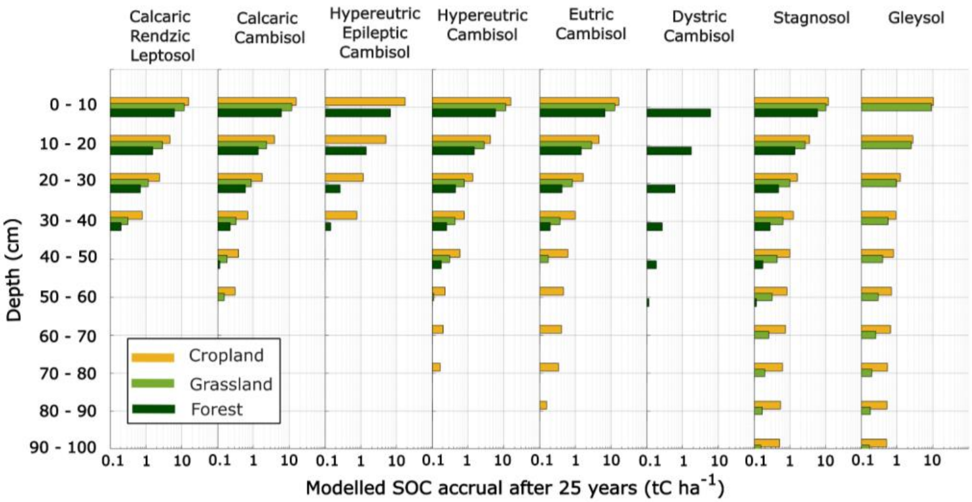


**Figure 5: Model results of SOC accrual after 25 years at each depth under the three considered C input scenarios (+1.5 tC ha$^{-1}$ y$^{-1}$ under croplands, +1.0 tC ha$^{-1}$ y$^{-1}$ under grasslands, +0.5 tC ha$^{-1}$ y$^{-1}$ under croplands compared to the ~~stationary~~ initial C inputs), t~~.~~ ~~T~~emperatures remaining constant. Model results for each soil type are only shown for the land uses represented in the dataset.**

### 3.3 Maps of SOC stocks, maximum ~~additional storage capacities~~SOC accrual, and simulated accrual after 25 years

The repartition of SOC stocks and maximum ~~additional storage capacities~~SOC accrual in the region of study is~~are~~ most visibly related to ~~the~~ land use, but is also affected by the spatial distribution of Stagnosols and Gleysols (Figure 6). The current SOC stock in the region of study amounts to a total of 3.9 MtC, with a standard deviation of 1.5 MtC according to the bootstrap method (Appendix ~~Figure 3~~I). To compare these results with national-scale estimates of SOC stocks, we average 3.9 MtC over the entire region of study and obtain a mean value of 122 tC ha$^{-1}$, of which 87 tC ha$^{-1}$ are in the first 30 cm.

The maximum SOC stocks that the region can theoretically contain is 3.9 + 2.5 = 6.4 MtC, suggesting that the soils in the region of study are at 61% of their theoretical maximum SOC stock. However, according to model results in ~~the chosen~~ scenario 3, this maximum SOC stock would only be reached over timescales of centuries to millenia, and the SOC accrual after 25 years only reaches 0.57 MtC. The SOC accrual in the region of study is attenuated by 14% and reaches 0.49 MtC when a 1.0 °C increase in temperature is implemented in the mineralization rates (Appendix J~~Figure 4~~).

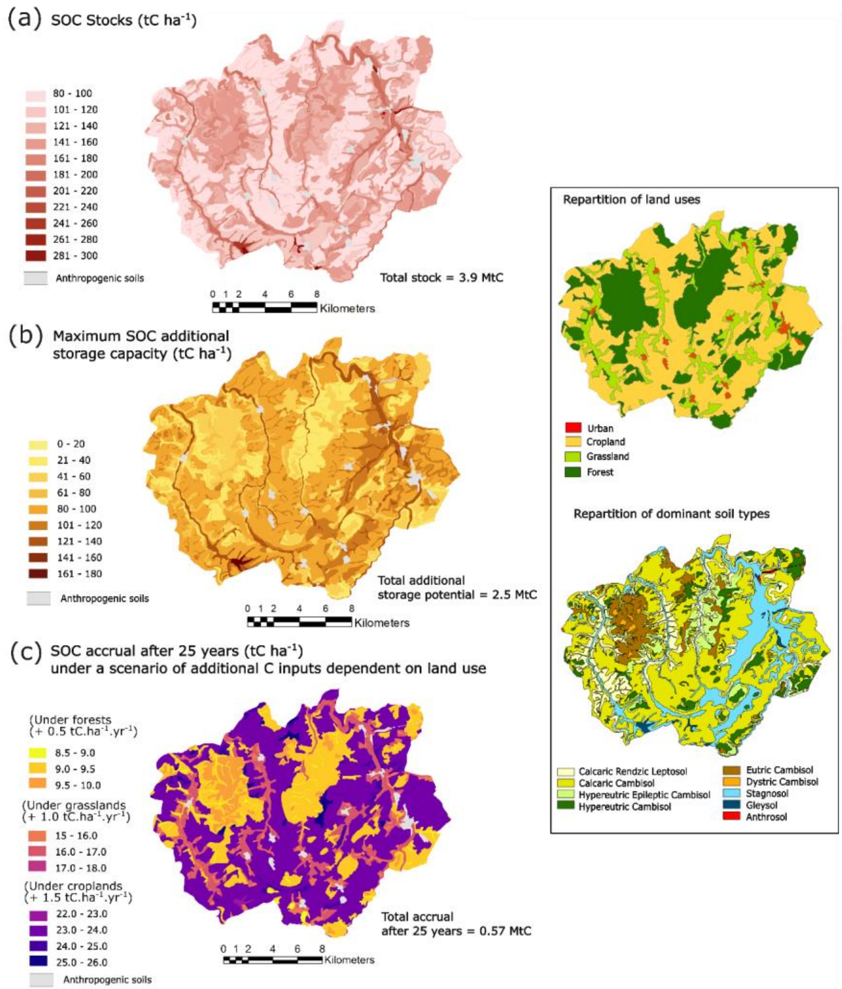

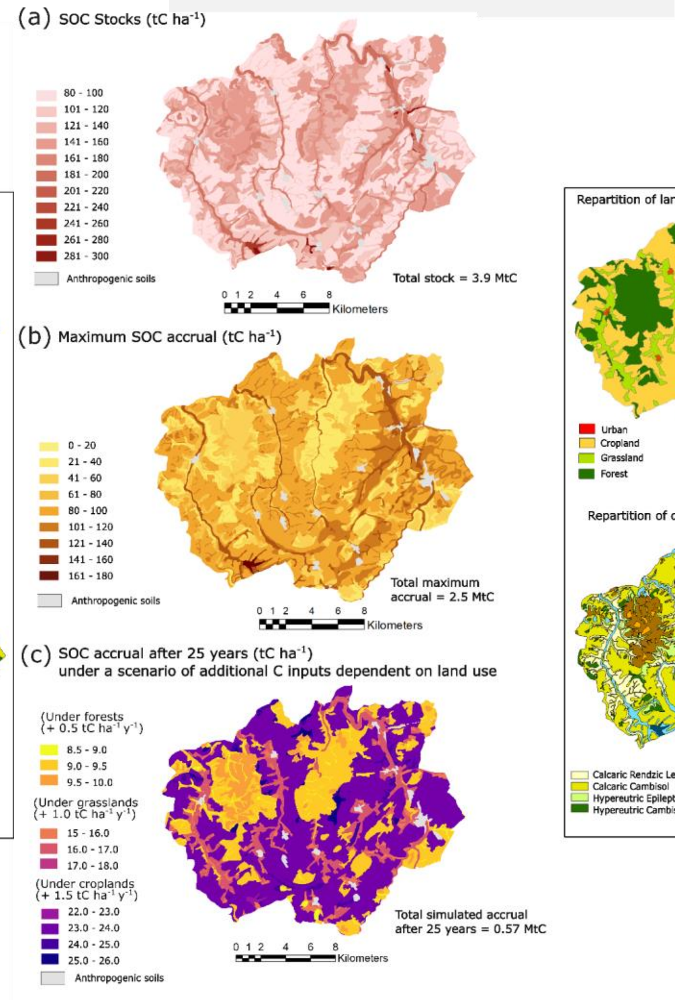


**Figure 6: Maps of SOC stocks (a), maximum SOC additional storage capacityaccrual (b) and simulated SOC accrual after 25 years under a realistic increased input scenario of additional C inputs compared to the steady state dependent on land use (+0.5 tC ha$^{-1}$ y$^{-1}$ under forests, +1.0 tC ha$^{-1}$ y$^{-1}$ under grassland, +1.5 tC ha$^{-1}$ y$^{-1}$ under cropland) (c). Upper and lower confidence intervals provided by the bootstrap method are given in Appendix Figure I3. The sStandard deviation of the total SOC stocks and additional storage potentialsmaximum SOC accrual based on the upper and lower confidence intervals applied to the whole region is 1.5 MtC.**

## 4 Discussion

### 4.1: Implications of our approaches to estimate target SOC stocks and accrual rates

There is a rising interest in representing the contribution of soils to carbon storage, both through the mapping of current SOC stocks, and through the mapping of the maximum SOC stocks that these soils can theoretically reach. used to explore the input rates and timescales needed to reach these targets SOC stocks. Our approach for estimating SOC theoretical maximum stocks was made possible by the uncommon abundance of soil profile data and by the detailed pedological map available in the region of study. This approach is most pertinent in areas where the land use and management has remained stable for many years (over 200 years in our region of study), because the high values of SOC stocks used to estimate target SOC stocks per soil type are more likely to represent a steady state rather than a transient stage. Such data-rich, well-documented regions can serve as references for similar pedoclimatic zones. A further step would then be to intensify profile-scale data collection in other regions to provide reference values of SOC stocks and maximum SOC accrual in as many pedoclimatic zones as possible, in order to upscale this approach from the regional to the global scale (Barré *et al.*, 2017).

Three C input scenarios were implemented to explore kinetics of SOC accrual. The first was an initial input regime obtained by matrix inversion, and corresponds to the annual C inputs necessary to maintain the initial SOC stocks at the steady state. We found a good agreement between the model-derived initial C inputs and available measurements and estimates made within the region of study: in croplands, the simulated C inputs were consistent with estimations of C inputs derived from the method of Bolinder *et al.* (2007) based on crop yields recorded in the region of study (Appendix K). In forests, the model-derived initial C inputs were consistent with measurements from the Renecofor carried out in the region of study.

The second scenario sought the annual C inputs necessary to reach the theoretical maximum SOC stocks within 25 years. The required annual C input rates largely exceed the realistic ranges from the literature for most soil types. The only soil types for which this scenario is realistic are the shallow soils (Calcaric Rendzic Leptosol and Hypereutric Epileptic Cambisol) and the sandy Dystric Cambisol, because these soils have lower SOC stocks than the others and are already close to their theoretical maximum SOC stocks.

The third scenario used realistic annual C input values from the literature, and found SOC accrual rates ranging from 0.32 – 1.04 tC $ha^{-1}$ $y^{-1}$ within the first 25 years. Examples can be found from previous studies of similar SOC accrual rates within decadal timescales following changes in land management strategies without changing the land use: transition from conventional to conservation agriculture in croplands (Autret *et al.*, 2016); promoting an increase in plant diversity in grasslands (Yang *et al.*, 2019); less frequent cutting in forests, or acting on forest productivity to increase root inputs and limiting soil disturbance during harvesting (Jandl *et al.*, 2007; Mayer *et al.*, 2020). The 1.5 tC $ha^{-1}$ $y^{-1}$ additional C inputs modelled in croplands resemble values calculated in a long-term field experiment after transition from conventional agriculture to conservation agriculture (1.72 tC $ha^{-1}$ $y^{-1}$ over 16 years, Autret *et al.*, 2016). Those inputs also correspond to what the model requires to maintain the theoretical maximum SOC stocks at steady state; this convergence confirms the robustness of the approach.

Using a percentile boundary line (here: 75th percentile of the SOC data) to estimate the theoretical maximum SOC stocks comes with a methodological challenge: the percentile regression necessarily depends on the size of the dataset and on its variability. A low percentile value within a large dataset underestimates the maximum SOC accrual, but an excessive percentile value within a small dataset produces an unrealistic target and increases the sensitivity to outliers. Other studies have used the following percentile values to estimate theoretical maximum SOC stocks at various spatial scales: Chen *et al.* (2019) compared maximum total SOC stocks following the 0.8, 0.85 and 0.9 percentile value at the national scale (1089 sites); Georgiou *et al.* (2022) compared the maximum mineral-associated SOC with low and high activity minerals at the 0.9, 0.95 and 0.975 percentiles at the global scale (1144 profiles). Standardized rules to define the choice of a percentile value for a target stock, depending on the scale of the study and the size and variability of the dataset, have yet to be established. Here, our choice of target SOC stocks at the 75th percentile is justified by the concordance between the annual C inputs necessary to maintain these stocks at steady state and realistic ranges of annual C inputs from Martin *et al.* (2021) and from regional Renecofor datasets (Table 2). By contrast, maintaining SOC stocks at the 88th percentile boundary line would require annual C inputs between 4.4 and 21.7 tC ha$^{-1}$ y$^{-1}$, far in excess of what can be realistically added to soils. We recommend, where possible, to verify the realism of SOC stock targets using carbon dynamics models and matrix inversion to estimate the annual C inputs necessary to reach these targets in the long term.

Interrogating the realism of target SOC stocks is of particular importance when deeper soil horizons are considered. Another concept used to define target SOC stocks is to focus on the mineral associated carbon, considered to be more stable, by using the clay and fine silt fraction as a proxy of the amount of carbon that can be theoretically stored in a soil in the long term (Hassink 1997, Cotrufo *et al.*, 2019, Georgiou *et al.*, 2022). However, applying this concept over the whole soil profile leads to unrealistically high targets, and therefore unrealistic C inputs at depth (Appendix L).

Modelled SOC accrual in scenario 3 ranged from 8.5 to 26 tC ha$^{-1}$ after 25 years, with a rapid decrease of SOC accrual rates with depth driven by decreasing C inputs. The deeper horizons of the soil provide limited opportunity for additional storage over short timescales using current land management practices. Furthermore, the proportion of new carbon inputs that is allocated to the fast carbon pool exceeds 85% at all depths in the soil profile (Appendix D): this implies that even in the deeper soil horizons, the majority of new C inputs is quickly mineralized, as also simulated by Sierra *et al.* (2024). The mean residence times (MRT) in the fast pool remain similar near the surface and at depth (17 – 38 years and 11 - 47 years respectively), but increase with depth in the slow pool (from 477 - 1100 years to 1744 - 5817 years). The greater contrast in mean residence times between the fast and slow pools at depth challenges our understanding of SOC dynamics.

across soil types are not sufficient to have a significant impact after 25 years, especially in the fast pool (Appendix D). It is rather the land use that affects SOC accrual by controlling the quantity and vertical repartition of inputs (Appendix E). However, soil type has a strong influence on current SOC stocks ~~to preserve~~ by categorizing soils based on profile depth, rock fragment content and other physico-chemical properties. Hydromorphic soils in particular have total SOC stocks up to three times higher

**Mis en forme :** Police :Gras, Couleur de police : Texte 1, Français (France) than in other soil types, making their preservation particularly critical. These high SOC stocks are due to waterlogged conditions strongly limiting decomposers activity (Sahrawat, 2004), notably for energetic reasons (Keiluweit *et al.*, 2016). Our model provides a widely-applicable tool to assess the effect of different soil types and initial distributions of SOC stocks on SOC dynamics at decadal timescales. It has yet to be validated with measures of SOC accrual in given land-use change pilots. The model does not [illegible] dynamics [illegible]. Further, the model does not account for vertical transport. Balesdent *et al.* (2018) showed that C incorporation in subsoil after a change in vegetation is slow and affects only long-term carbon dynamics. We can therefore consider that this process is negligible at decadal timescales. Sierra *et al.* (2024) also found that transport may only play a secondary role in the formation of soil carbon profiles according to simulation examples and measurements from carbon and radiocarbon profiles. ~~Finally, the p~~Priming effect is not taken into consideration in our model, even though it is expected to occur when C inputs to the soil increase, which could cause simulated results to overestimate SOC accrual (Guenet *et al.*, 2018). P~~But~~priming is difficult to include in predictive models because the processes involved are still poorly understood (Bernard *et al.*, 2022). Current explorations of the priming effect use either mechanistic models centred on microbial processes (Schimel, 2023), or theoretical models fitted to laboratory experiments, which do not fit the scope of our study.

Testing for the effect of temperature increase on mineralization rates led to an attenuation of SOC accrual by 2050 of 7 to 50 % depending on the climate scenario considered. We did~~, but our model could~~ not account holistically for the effects of climate change on SOC dynamics in this study~~:as they~~ t. ~~Those.~~The combination of changes in temperature, $CO_2$ concentration and precipitation can drive a myriad of responses in net primary production, SOC input repartition and mineralization processes (Rocci *et al.*, 2021; Bruni *et al.*, 2021). In forests for instance, increased drought conditions may increase tree mortality, but might also enhance deeper roots prospection for water, thereby changing the vertical repartition of C inputs (Schlesinger *et al.*, 2016). Different soil types are also expected to respond differently to climate change, due for instance to the impact of soil texture on soil moisture regimes (Bormann, 2012; Hartley *et al.*, 2021). Here, we have considered a simplified case where humidity conditions do not change from the 2009-2019 period and dot not affect soil carbon dynamics. The scientific community needs to improve its understanding of the priming effect, of SOC dynamics processes driven by climate change, and to further explore how soil type influences organic matter decomposition dynamics over decadal timescales.

### 4.2: Implications for stakeholders: what levels of C accrual are achievable after 25 years?

Increasing soil organic carbon (SOC) stocks in soils has the potential to provide global benefits, but its successful implementation requires regional scale information on land use and soil type. An important aspect of this work is to provide relevant SOC storage targets to stakeholders. The maximum SOC accrual can be used as a theoretical, long-term target value, but is not representative of how much carbon can realistically be added to soils over decadal timescales. In the region of study, total SOC accrual after 25 years under a realistic scenario of C inputs was found to be five times lower than the maximum theoretical SOC accrual (0.57 MgC versus 2.5 MgC), assuming no changes in the implemented practices increasing C inputs. Nevertheless, we observe that SOC accrual over 25 years is substantial. Our simulations of temperature following RCP4.5 (+1.0°C) and RCP8.5 (+1.3°C) attenuated this SOC accrual by 7 - 38% and 10 - 50% respectively over 25 years through the increase of mineralization rates. This shows that increasing organic matter inputs to the soil remains worthwhile, since SOC accrual remains significant even in an extreme scenario (highest projected increase in temperature but no change in humidity conditions). ~~**Tu peux peut etre mettre ici la notion evoquée précédemment sur l'effet humidité**~~

Maps of SOC stocks are efficient tools to synthetize scientific results at the regional scale for stakeholders. Crucially, they highlight areas where soil degradation would lead to the greatest release of $CO_2$. [illegible] SOC stocks [illegible] timescales of centuries to millennia, especially in the deeper soil horizons, but can be rapidly lost due to land use change and other disturbances. Therefore, as highlighted by Sierra *et al.* (2024), the priority should be to preserve the existing SOC stocks, even as we attempt to implement innovative land management practices to maximize these SOC stocks where possible. Despite the high uncertainties associated with regional-scale estimations of SOC stocks (Appendix I-J), our mean SOC stock values of 87 tC ha-1 in the first 30 cm are in accordance with national-scale estimates that found SOC stocks of 75 – 100 tC $ha^{-1}$ in the North-East of France (Pellerin *et al.*, 2021).

~~Maps of SOC stocks are efficient tools to synthetize scientific results at the regional scale for stakeholders. Crucially, they highlight areas where soil degradation would lead to the greatest release of $CO_2$.~~ The map of maximum SOC accrual was found to be of limited interest because it does not provide a timescale for when that maximum SOC stock might realistically be reached. Reaching the theoretical maximum SOC stocks by the 2050 horizon for carbon neutrality would require prohibitively high annual C input rates. We therefore recommend maps of prospective SOC accrual to be time-specific, with C input rates within realistic ranges.

Our time-specific SOC accrual map is an improvement from simple representation of maximum theoretical SOC stocks, but remains a simplification of what can realistically be implemented. The map implies a uniform increase in C input rates for each land use in the entire region of study, but this would likely be hindered by practical and socio-economic factors. The SOC stock and time-specific SOC accrual maps should be used as part of a wider set of decision support tools for land planners. In some circumstances, adding organic carbon to soils might not even be the best solution for mitigating climate change: biomass harvest not returned to the soils can instead be used as a source of food, biosourced energy or biomaterials (Derrien *et al.*, 2023). These alternate uses of carbon biomass offer a mean of substituting fossil carbon, which should be verified quantitatively by life cycle analysis.

Finally, soil type information provided to stakeholders should not be limited to the current or prospective SOC stocks. Soil-type specific physico-chemical properties are an important but as of yet poorly considered factor for land planning. Soil type affects numerous soil functions such as water retention, resistance to erosion and nutrient cycling (Adhikari & Hartemink, 2016). These soil functions should be considered in addition to the SOC dynamics to choose management strategies adapted to each soil type.

Informing stakeholders on soil management strategies to preserve and ~~maximise~~ maximize existing soil organic carbon (SOC) stocks is a pressing concern to the scientific community. It is critical to communicate on the effects of soil type, depth and land-use on SOC accrual in soil over time periods compatible with the roadmap for C neutrality~~. This study explored how~~

Mis en forme : Police :Non Gras, Couleur de police : Texte 1

Mis en forme : Police :Non Gras, Couleur de police : Texte 1

Mis en forme : Police :Non Gras, Couleur de police : Texte 1, Indice

Mis en forme : Police :Non Gras, Couleur de police : Texte 1 [illegible] The Hassink equation provided unrealistic profiles of SOC maximum additional storage capacity distribution at depth below 30 cm, as the equation only accounts for soil texture and does not consider the biotic controls on C inputs and SOC decomposition rates. Depth-dependent profiles of maximum SOC stocks estimated from the data-driven approach were more in line with what is known of root distribution and therefore C input distribution with depth.

We note a greater contrast of SOC mean residence times at depth, which invites further investigation: while a fraction of the new C inputs added to the deep soil horizons can remain stable over millennial timescales, the majority is mineralized within two decades. Simulating a rise in temperatures of 1.3°C over 25 years following RCP8.5 attenuated SOC accrual by 10 to 50%.

The effect of soil type on SOC mineralization rates was not visible over the decadal timescales considered. However, soil type plays an important role on the spatial repartition of the current SOC stocks that need to be preserved. Studies of SOC stocks and storage capacities should be complemented by more holistic explorations of soil functioning and ecosystem services which incorporate pedological knowledge.

This study provided a set of maps that give ato give a more complete picture of the issues related to carbon storage in soils (carbon stocks, maximum SOC accrualadditional storage capacities, and realisticpotentials for SOC accrual over decadal timescales). Such maps have the potential to facilitate communication with land planners and stakeholders by highlighting areas most worthy to preserve, and where carbon storage practices are likely to be the most efficient over decadal timescales. The efficacy of such maps as decision support tools should be explored via collaboration projects with stakeholders.

**Author contributions**

All authors have given approval to the final version of the manuscript. The manuscript was written through contributions of all authors as follows:

CHIROL Clémentine: Conceptualization; data analysis; SOC model development; original draft

SÉRÉ Geoffroy: Conceptualization; writing-review & editing

REDON Paul-Olivier: data provider; writing-review & editing

CHENU Claire: Conceptualization; writing-review & editing

DERRIEN Delphine: Conceptualization; SOC model advice and improvement; writing-review & editing

**Declaration of competing interest**

The authors declare that they have no known competing financial interests or personal relationships that could have appeared to influence the work reported in this paper.

## Acknowledgements

We received funding from the ANDRA, DEEPSURF and LUE for this project. We would like to thank Dr. Catherine Galy and Dr. Paul-Olivier Redon (ANDRA) for providing datasets and information on the OPE study area; Line Boulonne (RMQS) and Manuel Nicolas and Sébastien Macé (Renecofor) for providing datasets; and Dr. Laurent Saint-André and Dr. Marie-Pierre Turpault for their advice on the project.

## References

global-scale predictions of soil carbon stocks with Millennial Version 2. Soil Biology and Biochemistry, 164, 108466. https://doi.org/10.1016/j.soilbio.2021.108466

**Adhikari**, K., & Hartemink, A. E. (2016). Linking soils to ecosystem services — A global review. Geoderma, 262, 101–111. https://doi.org/10.1016/j.geoderma.2015.08.009

**Akpa**, S. I., Odeh, I. O., Bishop, T. F., Hartemink, A. E., & Amapu, I. Y. (2016). Total soil organic carbon and carbon sequestration potential in Nigeria. Geoderma, 271, 202-215. https://doi.org/10.1016/j.geoderma.2016.02.021

**Andriulo,** A., Mary, B., & Guerif, J. (1999) Modelling soil carbon dynamics with various cropping sequences on the rolling pampas. Agronomie 19:365–377. https://doi.org/10.1051/agro:19990504

**Autret**, B., Mary, B., Chenu, C., Balabane, M., Girardin, C., Bertrand, M., Grandeau, G., & Beaudoin, N. (2016). Alternative arable cropping systems: A key to increase soil organic carbon storage? Results from a 16 year field experiment. Agriculture, Ecosystems & Environment, 232, 150–164. https://doi.org/10.1016/j.agee.2016.07.008

**Balesdent**, J., Basile-Doelsch, I., Chadoeuf, J., Cornu, S., Derrien, D., Fekiacova, Z., & Hatté, C. (2018). Atmosphere–Soil Carbon Transfer as a Function of Soil Depth. Nature, 559(7715), 599–602. https://doi.org/10.1038/s41586-018-0328-3

**Barré**, P., Angers, D. A., Basile-Doelsch, I., Bispo, A., Cécillon, L., Chenu, C., Chevallier, T., Derrien, D., Eglin, T. K., & Pellerin, S. (2017). Ideas and perspectives: Can we use the soil carbon saturation deficit to quantitatively assess the soil carbon storage potential, or should we explore other strategies? Preprint Biogeosciences: Discussions. https://doi.org/10.5194/bg-2017-395

~~**Begill**, N., Don, A., & Poeplau, C. (2023). No detectable upper limit of mineral-associated organic carbon in temperate agricultural soils. Global Change Biology, 29, 4662–4669. https://doi.org/10.1111/gcb.16804~~

**Bormann**, H. (2012). Assessing the soil texture-specific sensitivity of simulated soil moisture to projected climate change by SVAT modelling. *Geoderma*, *185*, 73-83. https://doi.org/10.1016/j.geoderma.2012.03.021

**Code de champ modifié**

**Bruni**, E., Guenet, B., Huang, Y., Clivot, H., Virto, I., Farina, R., ... & Chenu, C. (2021). Additional carbon inputs to reach a 4 per 1000 objective in Europe: Feasibility and projected impacts of climate change based on Century simulations of long-term arable experiments. Biogeosciences, 18(13), 3981-4004.

**Chen**, S., Martin, M. P., Saby, N. P., Walter, C., Angers, D. A., & Arrouays, D. (2018). Fine resolution map of top and subsoil carbon sequestration potential in France. Science of the Total Environment, 630, 389-400. https://doi.org/10.1016/j.scitotenv.2018.02.209

**Chen**, S., Arrouays, D., Angers, D. A., Martin, M. P., & Walter, C. (2019b). Soil carbon stocks under different land uses and the applicability of the soil carbon saturation concept. Soil and Tillage Research, 188, 53-58. https://doi.org/10.1016/j.still.2018.11.001

**Cotrufo**, M. F., Ranalli, M. G., Haddix, M. L., Six, J., & Lugato, E. (2019). Soil carbon storage informed by particulate and mineral-associated organic matter. Nature Geoscience, 12(12), 989–994. https://doi.org/10.1038/s41561-019-0484-6

**Cotrufo**, M. F., & Lavallee, J. M. (2022). Soil organic matter formation, persistence, and functioning: A synthesis of current understanding to inform its conservation and regeneration. Advances in agronomy, 172, 1-66. https://doi.org/10.1016/bs.agron.2021.11.002

**De Vos**, B., Cools, N., Ilvesniemi, H., Vesterdal, L., Vanguelova, E., & Carnicelli, S. (2015). Benchmark values for forest soil carbon stocks in Europe: Results from a large scale forest soil survey. Geoderma, 251–252, 33–46. https://doi.org/10.1016/j.geoderma.2015.03.008

**Don**, A., Seidel, F., Leifeld, J., Kätterer, T., Martin, M., Pellerin, S., Emde, D., Seitz, D., & Chenu, C. (2023). Carbon sequestration in soils and climate change mitigation—Definitions and pitfalls. Global Change Biology, 00, e16983. https://doi.org/10.1111/gcb.16983

**Feng**, W., Plante, A. F., & Six, J. (2013). Improving estimates of maximal organic carbon stabilization by fine soil particles. Biogeochemistry, 112, 81–93. https://doi.org/10.1007/s10533-011-9679-7

**Gross**, C. D., & Harrison, R. B. (2019). The case for digging deeper: Soil organic carbon storage, dynamics, and controls in our changing world. Soil Systems, 3, 28. https://doi.org/10.3390/soilsystems3020028

**Guo**, L. B., & Gifford, R. M. (2002). Soil carbon stocks and land use change: a meta analysis. Global change biology, 8(4), 345-360, https://doi.org/10.1046/j.1354-1013.2002.00486.x

**Harrison**, R. B., Footen, P. W., & Strahm, B. D. (2011). Deep soil horizons: Contribution and importance to soil carbon pools and in assessing whole-ecosystem response to management and global change. Forest Science, 57(1), 67–76. https://doi.org/10.1093/forestscience/57.1.67

**Hartley**, I. P., Hill, T. C., Chadburn, S. E., & Hugelius, G. (2021). Temperature effects on carbon storage are controlled by soil stabilisation capacities. Nature Communications, 12(1), 6713. https://doi.org/10.1038/s41467-021-27101-1

**Hassink**, J. (1997). The capacity of soils to preserve organic C and N by their association with clay and silt particles. Plant and Soil, 191, 77–87. https://doi.org/10.1023/A:1004213929699

**Code de champ modifié**

**Houot**, S., Pons, M.-N., Pradel, M., Savini, I., & Tibi, A. (n.d.). Valorisation des matières fertilisantes d'origine résiduaire sur les sols à usage agricole ou forestier. INRA.

**Jackson**, R. B., Canadell, J., Ehleringer, J. R., Mooney, H. A., Sala, O. E., & Schulze, E. D. (1996). A global analysis of root distributions for terrestrial biomes. Oecologia, 108(3), 389–411. https://doi.org/10.1007/BF00333714

**Jandl**, R., Lindner, M., Vesterdal, L., Bauwens, B., Baritz, R., Hagedorn, F., ... Minkkinen, K. (2007). How strongly can forest management influence soil carbon sequestration? Geoderma, 137, 253–268. https://doi.org/10.1016/j.geoderma.2006.09.003

**Jobbágy**, E. G., & Jackson, R. B. (2000). The vertical distribution of soil organic carbon and its relation to climate and vegetation. Ecological Applications, 10(2), 423–436. https://doi.org/10.1890/1051-0761(2000)010[0423:TVDOSO]2.0.CO;2

**Jreich**, R. (2018). Vertical dynamics of soil carbon: Combined use of isotopic tracers and statistical meta-analysis (PhD thesis). Université Paris-Saclay.

**Keiluweit**, M., Nico, P. S., Kleber, M., & Fendorf, S. (2016). Are oxygen limitations under recognized regulators of organic carbon turnover in upland soils? Biogeochemistry, 127(2–3), 157–171. https://doi.org/10.1007/s10533-015-0180-6

**Kögel-Knabner**, I., & Amelung, W. (2021). Soil organic matter in major pedogenic soil groups. Geoderma, 384, 114785. https://doi.org/10.1016/j.geoderma.2020.114785

**Lal**, R. (2005). Forest soils and carbon sequestration. Forest Ecology and Management, 220(1–3), 242–258. https://doi.org/10.1016/j.foreco.2005.08.015

**Levavasseur**, F., Mary, B., Christensen, B. T., Duparque, A., Ferchaud, F., Kätterer, T., Lagrange, H., Montenach, D., Resseguier, C. & Houot, S. (2020). The simple AMG model accurately simulates organic carbon storage in soils after repeated application of exogenous organic matter. Nutrient Cycling in Agroecosystems, 117, 215–229. https://doi.org/10.1007/s10705-020-10065-x

**Luo**, Z., Feng, W., Luo, Y., Baldock, J., & Wang, E. (2017). Soil organic carbon dynamics jointly controlled by climate, carbon inputs, soil properties and soil carbon fractions. *Global change biology*, *23*(10), 4430-4439. https://doi.org/10.1111/gcb.13767

**Malik**, A. A., Puissant, J., Buckeridge, K. M., Goodall, T., Jehmlich, N., Chowdhury, S., ... Banfield, J. F. (2018). Land use driven change in soil pH affects microbial carbon cycling processes. Nature Communications, 9(1), 3591. https://doi.org/10.1038/s41467-018-05980-1

**Martin**, M. P., Dimassi, B., Román Dobarco, M., Guenet, B., Arrouays, D., Angers, D. A., ... & Pellerin, S. (2021). Feasibility of the 4 per 1000 aspirational target for soil carbon: A case study for France. Global Change Biology, 27(11), 2458-2477. https://doi.org/10.1111/gcb.15547

**Mary**, B., Beaudoin, N., Justes, E., & Machet, J. M. (1999). Calculation of nitrogen mineralization and leaching in fallow soil using a simple dynamic model. European Journal of Soil Science, 50, 549–566. https://doi.org/10.1046/j.1365-2389.1999.00264.x

climate: A worldwide meta-analysis of radiocarbon profiles. Global Change Biology, 21, 4278–4292. https://doi.org/10.1111/gcb.13012

**Mayer**, M., Prescott, C. E., Abaker, W. E., Augusto, L., Cécillon, L., Ferreira, G. W., ... Vesterdal, L. (2020). Influence of forest management activities on soil organic carbon stocks: A knowledge synthesis. Forest Ecology and Management, 466, 118127.

**Minasny**, B., Malone, B. P., McBratney, A. B., Angers, D. A., Arrouays, D., Chambers, A., ... Winowiecki, L. (2017). Soil carbon 4 per mille. Geoderma, 292, 59–86. https://doi.org/10.1016/j.geoderma.2017.01.002

**Party**, J. P., Vauthier, Q., & Rigou, L. (2019). Notice de la carte pédologique au 1/50000 de la zone OPE.

**Pellerin**, S., Bamière, L., Savini, I., Rechauchère, O., Launay, C., Martin, R., Schiavo, M., Angers, D., Augusto, L., Balesdent, J., Basile-Doelsch, I., Bellassen, V., Cardinael, R., Cécillon, L., Ceschia, E., Chenu, C., Constantin, J., Daroussin, J., Delacote, P., Delame, N., Gastal, F., Gilbert, D., Graux, A.-I., Guenet, B., Houot, S., Klumpp, K., Letort, E., Litrico, I., Martin, M., Menasseri-Aubry, S., Meziere, D., Morvan, T., Mosnier, C., Roger-Estrade, J., Saint-André, L., Sierra, J., Therond, O., Viaud, V., & Grateau, R., Le Perchec, S. (2021). Stocker du carbone dans les sols français.

[illegible] Global Change Biology, 30(8), e17453. https://doi.org/10.1111/gcb.17453

**Rocci**, K. S., Lavallee, J. M., Stewart, C. E., & Cotrufo, M. F. (2021). Soil organic carbon response to global environmental change depends on its distribution between mineral-associated and particulate organic matter: A meta-analysis. Science of the Total Environment, 793, 148569. https://doi.org/10.1016/j.scitotenv.2021.148569

**Rowley**, M. C., Grand, S., Spangenberg, J. E., & Verrecchia, E. P. (2021). Evidence linking calcium to increased organo-mineral association in soils. Biogeochemistry, 153(3), 223–241. https://doi.org/10.1007/s10533-021-00779-7

**Saffih-Hdadi**, K. & Mary, B. (2008). Modeling consequences of straw residues export on soil organic carbon. Soil Biol Biochem 40:594–607. https://doi.org/10.1016/j.soilbio.2007.08.022

**Saxton**, K. E., & Rawls, W. J. (2006). Soil water characteristic estimates by texture and organic matter for hydrologic solutions. Soil science society of America Journal, 70(5), 1569-1578. https://doi.org/10.2136/sssaj2005.0117

**Schimel**, J. (2023). Modeling ecosystem-scale carbon dynamics in soil: the microbial dimension. Soil Biology and Biochemistry, 178, 108948. https://doi.org/10.1016/j.soilbio.2023.108948

**Schweizer**, S. A. (2022). Perspectives from the Fritz-Scheffer Awardee 2021: Soil organic matter storage and functions determined by patchy and piled-up arrangements at the microscale. Journal of Plant Nutrition and Soil Science, 185(6), 694-706. **Sierra**, C. A., Ahrens, B., Bolinder, M. A., Braakhekke, M. C., von Fromm, S., Kätterer, T., ... Wang, G. (2024). Carbon sequestration in the subsoil and the time required to stabilize carbon for climate change mitigation. Global Change Biology, 30(1), e17153.

**Soubeyroux**, J.-M., Bernus, S., Corre, L., Drouin, A., Dubuisson, B., Etchevers, P., Gouget, V., Josse, P., Kerdoncuff, M., Samacoits, R., & Tocquer, F. (2020) Les nouvelles projections climatiques de référence DRIAS 2020 pour la métropole. Météo-France. **Shiri**, J., Keshavarzi, A., Kisi, O., Karimi, S., & Iturraran-Viveros, U. (2017). Modeling soil bulk density through a complete data scanning procedure: Heuristic alternatives. Journal of Hydrology, 549, 592-602. https://doi.org/10.1016/j.jhydrol.2017.04.035

**Sierra**, C. A., Ahrens, B., Bolinder, M. A., Braakhekke, M. C., von Fromm, S., Kätterer, T., ... Wang, G. (2024). Carbon sequestration in the subsoil and the time required to stabilize carbon for climate change mitigation. Global Change Biology, 30(1), e17153.

**Verma**, Y., Singh, N. K., & Pathak, S. O. (2017). Application of carbon isotopic techniques in the study of soil organic matter dynamics. International Journal of Chemical Studies, 5(6), 1123–1128.

**Wiesmeier**, M., Von Lützow, M., Spörlein, P., Geuß, U., Hangen, E., Reischl, A., ... Kögel-Knabner, I. (2015). Land use effects on organic carbon storage in soils of Bavaria: The importance of soil types. Soil and Tillage Research, 146, 296–302. https://doi.org/10.1016/j.still.2014.10.003

**Yang**, Y., Tilman, D., Furey, G., & Lehman, C. (2019). Soil carbon sequestration accelerated by restoration of grassland biodiversity. Nature Communications, 10(1), 718. https://doi.org/10.1038/s41467-019-08636-w

## Appendices

### Appendix A: List of soil properties collected at each soil profile and their measurement protocol

| Study type | Soil Property | Unit | Method |
|---|---|---|---|
| Field observation | Slope | % | In situ operator's assessment |
| | Soil depth | Cm | In situ operator's assessment |
| | Horizon Textural Class | Type | In situ operator's assessment completed by NF X 31-107 |
| | Horizon Compacity | Type | knife test (ISO 25177: 2008) |
| | Horizon Rock Fragment Content | % | In situ operator's assessment |
| | Horizon Hydromorphic Features | Type | In situ operator's assessment |
| Lab Agronomical Analysis | Horizon pH | - | NF ISO 10390 |
| | Horizon OM | g/kg | NF ISO 10694 |
| | Horizon CaCO3 | g/kg | NF ISO 10693 |

### Appendix B~~Table 2~~: List of descriptors used to plot the SOC content curves for each soil type and land use: $\Omega_1$ the SOC content of the soil type at maximal depth, $\Omega_2$ the SOC content at the surface, and $\Omega_3$ the depth at half maximum of the SOC content (based on Mathieu ~~et al.~~*et al.* (2015) and Jreich (2018))

| Land use | Soil type (WRB) | Soil type (RPF) | $\Omega_1$ Bottom SOC (g/kg) | $\Omega_2$ Top SOC (g/kg) | $\Omega_3$ Depth at half maximum of the carbon content (cm) |
|---|---|---|---|---|---|
| Cropland | Calcaric rendzic leptosol | Rendosol | 17 | 31 | 17 |
| Forest | Calcaric rendzic leptosol | Rendosol | 22 | 74 | 16 |
| Grassland | Calcaric rendzic leptosol | Rendosol | 12 | 53 | 15 |
| Cropland | Calcaric cambisol | Calcosol | 14 | 33 | 21 |
| Forest | Calcaric cambisol | Calcosol | 17 | 62 | 18 |
| Grassland | Calcaric cambisol | Calcosol | 14 | 54 | 15 |
| Cropland | Hypereutric epileptic cambisol | Rendisol | 19 | 38 | 13 |
| Forest | Hypereutric epileptic cambisol | Rendisol | 16 | 60 | 12 |
| Cropland | Hypereutric cambisol | Calcisol | 10 | 24 | 17 |
| Forest | Hypereutric cambisol | Calcisol | 22 | 64 | 21 |
| Grassland | Hypereutric cambisol | Calcisol | 14 | 54 | 15 |
| Cropland | Eutric cambisol | Brunisol | 8 | 18 | 21 |

| | | | | | |
|---|---|---|---|---|---|
| Forest | Eutric cambisol | Brunisol | 8 | 45 | 16 |
| Grassland | Eutric cambisol | Brunisol | 5 | 23 | 21 |
| Forest | Dystric cambisol | Alocrisol | 4 | 31 | 15 |
| Cropland | Stagnosol | Rédoxisol | 10 | 21 | 19 |
| Forest | Stagnosol | Rédoxisol | 9 | 46 | 17 |
| Grassland | Stagnosol | Rédoxisol | 9 | 40 | 14 |
| Cropland | Gleysol | Réductisol | 16 | 26 | 16 |
| Grassland | Gleysol | Réductisol | 21 | 68 | 18 |

Mis en forme : Police :(Par défaut) +Corps (Times New Roman), 8 pt

Mis en forme : Police :(Par défaut) +Corps (Times New Roman), 8 pt

Mis en forme : Police :(Par défaut) +Corps (Times New Roman), 8 pt

Mis en forme : Police :(Par défaut) +Corps (Times New Roman), 8 pt

Mis en forme : Police :(Par défaut) +Corps (Times New Roman), 8 pt

Mis en forme : Police :(Par défaut) +Corps (Times New Roman), 8 pt

Mis en forme : Police :(Par défaut) +Corps (Times New Roman), 8 pt

Mis en forme : Police :(Par défaut) +Corps (Times New Roman), 8 pt

**Appendix C~~1~~: Details of model functioning**

A depth-dependent SOC dynamic model using multilayer soil modules was built to establish the time needed to reach different levels of carbon storage in the soil. SOC is allocated to three boxes (fast, slow, stable) corresponding to different SOC mineralization rates defined by Balesdent ~~*et al.*~~*et al.* (2018) based on a meta-analysis of changes in stable carbon isotope signatures at 55 grassland, forest and cropland sites, in the tropical zone. ~~The mineralization rates were obtained using a $C_3/C_4$ approach, which is typically efficient to follow carbon dynamics over timescales ranging from one to one thousand years. Compared to the $^{14}C$ method, which covers timescales of several thousand years, the $C_3/C_4$ approach is relevant for land planning by exploring the impact of land use change on SOC dynamics (Verma *et al.*, 2017).~~

The mineralization factors associated with each box were then corrected for temperate soils using correction factors defined for the AMG model to account for the difference in environmental conditions (temperature and humidity) between tropical and temperate, but also to account for the differences in pH, clay content and $CaCO_3$ between soil types. The correction factors linked to temperature and humidity ~~were~~ are based on~~based on~~ Andriulo *et al.* (1999) and Saffih-Hdadi and Mary (2008)~~Mary *et al.* (1999)~~. The correction factors linked to pH, clay content and $CaCO_3$ were previously established by Clivot ~~*et al.*~~*et al.* (2017) based on the monitoring of N mineralization in 65 bare fallow soils representative of arable cropping systems in France, over a depth up to 150cm. These corrections are in accordance with recommendations from Rasmussen ~~*et al.*~~*et al.* (2018), for whom SOM stabilization not only depends on clay content, but also on pH and exchangeable calcium for alkaline soils. The correction factors for the temperature (T), humidity (H), clay content (A), pH and $CaCO_3$, as used in the 2019 AMG model, were as follows:

- $fT = \frac{25}{1+(25-1) * e^{0.12*15} * e^{-0.12*T}}$ *[~~Appendix~~ Equation C1]*
- $fH = \frac{1}{1+0.03*e^{-5.247*(P-PET)/1000}}$ *[Equation C2~~Appendix Equation 2~~]*
- $fA = e^{-2.519 * 10^{-3} * Clay}$ *[Equation C~~Appendix Equation~~ 3]*
- $fpH = e^{-0.112 * (pH-8.5)^2}$ *[Equation C~~Appendix Equation~~ 4]*
- $fCaCO_3 = \frac{1}{1+(1.5*10^{-3} * CaCO3)}$ *[Equation C~~Appendix Equation~~ 5]*

With T the mean annual temperature, P the mean annual precipitation and PET the potential evapotranspiration.

The total correction factor f = fT * fH * fA * fpH * $fCaCO_3$, was calculated for ~~both~~ the ~~55~~ tropical sites from Balesdent ~~*et al.*~~ *et al.* (2018) and for the temperate conditions in the OPE region of the study (~~,~~ $f_{BAL}$ and $f_{OPE}$ respectively). The corrected mineralization factors $k1_{corr}$ and $k2_{corr}$ were obtained with the following equations:

- $k1_{corr} = k1 * f_{OPE} / f_{BAL}$ *[Equation C~~Appendix Equation~~ 6]*
- $k2_{corr} = k2 * f_{OPE} / f_{BAL}$ *[Equation C~~Appendix Equation~~ 7]*

For each soil type and land use, the initial carbon stocks every 10 cm ~~($C_{init}$)~~ was again obtained by data interpolation with the Jreich method (2018); they were distributed between the three ~~boxes~~ pools based on the depth-dependent allocation factors defined by Balesdent ~~*et al.*~~ *et al.* (2018) ~~(a1 and a2)~~, as follows:

- $C1_{init}(i) = C_{init}(i) * a1(i)$ *[Equation C~~Appendix Equation~~ 8]*
- $C2_{init}(i) = C_{init}(i) * a2(i)$ *[Equation C~~Appendix Equation~~ 9]*
- $C3_{init}(i) = C_{init}(i) * (1-(a1(i)+a2(i)))$ *[Equation C~~Appendix Equation~~ 10]*

With $C_{init}$ the initial carbon stock, and a1 and a2 the ~~allocation factors~~ proportion of carbon in ~~to~~ pool 1 and 2 at each depth i.

The incorporated soil carbon inputs at each depth i and timestep t were added as follows:

- $C1_{in}(t,i) = INPUT(i) * \alpha(i)$ *[Equation C~~Appendix Equation~~ 11]*
- $C2_{in}(t,i) = INPUT(i) * (1-\alpha(i))$ *[Equation C~~Appendix Equation~~ 12]*

with α the proportion of new carbon inputs that is allocated to the fast carbon pool, calculated from the steady-state input equations (see Equations C19-22 below).

With $\alpha(i) = \frac{\frac{a1*k1corr}{a2*k2corr}}{1+(\frac{a1*k1corr}{a2*k2corr})}$ *[Appendix Equation 13]*

- $C1_{out}(t,i)=C1(t,i) * ( e^{-k1_{corr}(i)*timestep} - 1)$ *[Equation C13Appendix Equation 14]*
- $C2_{out}(t,i)=C2(t,i) * ( e^{-k2_{corr}(i)*timestep} - 1)$ *[Equation C14Appendix Equation 15]*

The change in soil carbon stock at each depth i between t and t+1 was defined as follows:

- $dC1(t,i)=C1_{out}(t,i) + C1_{in}(t,i)$ *[Equation C15Appendix Equation 16]*
- $dC2(t,i)=C1_{out}(t,i) + C2_{in}(t,i)$ *[Equation C16Appendix Equation 17]*

The soil carbon stocks at t+1 were therefore defined as:

- $C1(t+1,i) = C1(t,i) + dC1(t,i)$ *[Equation C17Appendix Equation 18]*
- $C2(t+1,i) = C2(t,i) + dC2(t,i)$ *[Equation C18Appendix Equation 19]*

The corrected mineralization rates also led to the definition of carbon mean residence times as a function of depth for each soil type (MRT = 1/k, see Appendix BTable 2). SOC mean residence times at the steady state depend on the physico-chemical properties of the studied soil types: in our study site, they range from 50 – 100 years in the topsoil and from 145 – 453 years underneath.

The model was initialized under the assumption that the carbon stocks calculated at the different depths in 2018 were at steady state. This assumption is justified on average by a land occupation map from 1830 showing limited changes in land use over the past 200 years (Dupouey *et al.et al.*, 2008). Inversing the model at the steady state yielded the vertical repartition of yearly C inputs necessary to keep the input and output fluxes equal across the full profile (Derrien & Amelung, see Appendix table 2 and Appendix Figure 1). We defined $INPUT_{eq}$ the repartition of incorporated C inputs every 10 cm at the steady state, as follows:

- $C1_{eq}(i) = INPUT(i) * \frac{\alpha(i)}{k1_{corr}}$ *[Equation CAppendix Equation 1920]*
- $C2_{eq}(i) = INPUT(i) * \frac{(1-\alpha)}{k2_{corr}}$ *[Equation CAppendix Equation 201]*

The two previous equations are used to define α as follows:

- $\alpha(i) = \frac{\frac{a1*k1corr}{a2*k2corr}}{1+(\frac{a1*k1corr}{a2*k2corr})}$ *[Equation C21]*

assumed that there was no vertical redistribution of SOC between the layers following this initial allocation (Balesdent ~~et al.~~*et al.*, 2018). Then, the allocation and mineralization rates of these inputs were used at each depth layer to infer the mean residence time of the C inputs per land use: this second definition of the mean residence time depends on both the physico-chemical properties of the soil and on the vertical repartition of inputs.

~~**Appendix Table 1: List of soil properties collected at each soil profile and their measurement protocol**~~

| **Depth (cm)** | **a1**~~α~~ ~~0.98 0.92 0.86~~ | **a2**~~0.86 0.88 0.90 0.91~~ | ***α*** ~~0.91 0.91 0.92~~ | ~~**Average**~~ **Mean Residence Time MRT (y)** | | | | | | | | | | | | | | | |
|---|---|---|---|---|---|---|---|---|---|---|---|---|---|---|---|---|---|---|---|
| | | | | **Soil 1** | | **Soil 2** | | **Soil 3** | | **Soil 4** | | **Soil 5** | | **Soil 6** | | **Soil 7** | | **Soil 8** | |
| | | | | MRT1 | MRT2 | MRT1 | MRT2 | MRT1 | MRT2 | MRT1 | MRT2 | MRT1 | MRT2 | MRT1 | MRT2 | MRT1 | MRT2 | MRT1 | MRT2 |
| 0–10 | 0,61 | 0,34 | 0.98 | 22 | 628 | 20 | 563 | 22 | 630 | 20 | 566 | 26 | 742 | 38 | 1100 | 23 | 664 | 17 | 477 |
| 10–20 | 0,29 | 0,67 | 0.92 | 31 | 777 | 27 | 696 | 31 | 779 | 28 | 701 | 36 | 918 | 37 | 948 | 32 | 822 | 23 | 591 |
| 20–30 | 0,11 | 0,85 | 0.86 | 13 | 643 | 14 | 676 | 26 | 1284 | 23 | 1121 | 29 | 1422 | 24 | 1190 | 21 | 1031 | 15 | 741 |
| 30–40 | 0,07 | 0,86 | 0.86 | 13 | 863 | 13 | 908 | 25 | 1724 | 22 | 1505 | 28 | 1910 | 25 | 1727 | 14 | 977 | 13 | 892 |
| 40–50 | 0,07 | 0,83 | 0.88 | | | 11 | 1013 | 26 | 2321 | 23 | 2026 | 29 | 2571 | 22 | 1943 | 15 | 1315 | 14 | 1200 |
| 50–60 | 0,07 | 0,80 | 0.90 | | | 13 | 1317 | | | 44 | 4654 | 30 | 3198 | 24 | 2526 | 16 | 1710 | 15 | 1561 |
| 60–70 | 0,07 | 0,75 | 0.91 | | | | | | | 47 | 5171 | 32 | 3553 | 25 | 2807 | 17 | 1900 | 16 | 1734 |
| 70–80 | 0,05 | 0,71 | 0.91 | | | | | | | 42 | 5817 | 29 | 3997 | 23 | 3158 | 14 | 1948 | 14 | 1951 |
| 80–90 | 0,04 | 0,65 | 0.91 | | | | | | | 37 | 5817 | 26 | 3997 | 20 | 3158 | 12 | 1948 | 11 | 1744 |
| 90–100 | 0,04 | 0,60 | 0.92 | | | | | | | | | | | 22 | 3501 | 12 | 1948 | 11 | 1744 |
| **Average MRT above 30 cm** | | | | 62 | | 57 | | 69 | | 62 | | 81 | | 100 | | 70 | | 50 | |
| **Average MRT below 30 cm** | | | | 145 | | 155 | | 309 | | 453 | | 418 | | 384 | | 226 | | 206 | |

**Appendix E~~Table 4~~: Vertical repartition in % of yearly C inputs at the steady state ~~(stationary C inputs)~~ for each soil type, land use and depth layer every 10 cm. The bottom of the table provides the total inputs in tC ha$^{-1}$ y$^{-1}$ needed to stay at the steady state, or to reach the maximum SOC stocks estimated by the 75$^{th}$ percentile data-driven method. C = Cropland; F = Forest; G = Grassland.**

| Depth (cm) | Calcaric rendzic leptosol | | | Calcaric cambisol | | | Hypereutric epileptic cambisol | | Hypereutric cambisol | | | Eutric cambisol | | | Dystric cambisol | Stagnosol | | | Gleysol | |
|---|---|---|---|---|---|---|---|---|---|---|---|---|---|---|---|---|---|---|---|---|
| | C | F | G | C | F | G | C | F | C | F | G | C | F | G | F | C | F | G | C | G |
| 0 | 0.672 | 0.709 | 0.737 | 0.701 | 0.700 | 0.764 | 0.739 | 0.772 | 0.705 | 0.699 | 0.743 | 0.668 | 0.738 | 0.760 | 0.629 | 0.499 | 0.651 | 0.630 | 0.489 | 0.606 |
| 10 | 0.173 | 0.167 | 0.158 | 0.148 | 0.155 | 0.128 | 0.184 | 0.172 | 0.164 | 0.171 | 0.154 | 0.160 | 0.157 | 0.151 | 0.174 | 0.130 | 0.149 | 0.142 | 0.108 | 0.141 |
| 20 | 0.116 | 0.096 | 0.082 | 0.082 | 0.083 | 0.060 | 0.045 | 0.034 | 0.054 | 0.055 | 0.046 | 0.061 | 0.049 | 0.045 | 0.061 | 0.066 | 0.060 | 0.060 | 0.056 | 0.061 |
| 30 | 0.039 | 0.028 | 0.023 | 0.033 | 0.031 | 0.023 | 0.030 | 0.020 | 0.032 | 0.032 | 0.025 | 0.037 | 0.023 | 0.020 | 0.025 | 0.058 | 0.041 | 0.044 | 0.043 | 0.037 |
| 40 | | | | 0.020 | 0.018 | 0.014 | 0.003 | 0.002 | 0.024 | 0.023 | 0.018 | 0.023 | 0.012 | 0.010 | 0.019 | 0.047 | 0.026 | 0.030 | 0.038 | 0.026 |
| 50 | | | | 0.015 | 0.013 | 0.011 | | | 0.008 | 0.007 | 0.005 | 0.017 | 0.008 | 0.005 | 0.013 | 0.038 | 0.017 | 0.021 | 0.033 | 0.019 |
| 60 | | | | | | | | | 0.007 | 0.006 | 0.005 | 0.015 | 0.006 | 0.004 | 0.011 | 0.034 | 0.013 | 0.017 | 0.030 | 0.016 |
| 70 | | | | | | | | | 0.006 | 0.005 | 0.004 | 0.013 | 0.005 | 0.003 | 0.009 | 0.030 | 0.010 | 0.014 | 0.026 | 0.013 |
| 80 | | | | | | | | | 0.002 | 0.002 | 0.001 | 0.006 | 0.002 | 0.001 | 0.009 | 0.029 | 0.009 | 0.013 | 0.028 | 0.013 |
| 90 | | | | | | | | | | | | | | | 0.008 | 0.027 | 0.009 | 0.012 | 0.027 | 0.013 |
| 100 | | | | | | | | | | | | | | | 0.009 | 0.030 | 0.010 | 0.013 | 0.031 | 0.014 |
| 110 | | | | | | | | | | | | | | | 0.009 | 0.012 | 0.004 | 0.005 | 0.031 | 0.014 |
| 120 | | | | | | | | | | | | | | | 0.009 | | | | 0.031 | 0.014 |
| 130 | | | | | | | | | | | | | | | 0.009 | | | | 0.028 | 0.013 |
| 140 | | | | | | | | | | | | | | | 0.009 | | | | | |
| Total inputs to stay at the steady state (tC ha$^{-1}$ y$^{-1}$) | 1.34 | 2.75 | 1.91 | 1.84 | 2.83 | 2.73 | 1.47 | 1.97 | 1.36 | 2.26 | 2.51 | 0.98 | 2.02 | 1.19 | 1.03 | 1.50 | 2.33 | 1.92 | 2.79 | 4.59 |
| Total inputs to reach Max SOC (tC ha$^{-1}$ y$^{-1}$) | 3.15 | 3.61 | 2.20 | 3.14 | 2.26 | 1.44 | 3.22 | 5.99 | 3.15 | 3.61 | 2.20 | 3.14 | 2.26 | 1.44 | 3.22 | 5.99 | 3.15 | 3.61 | 2.20 | 3.14 |

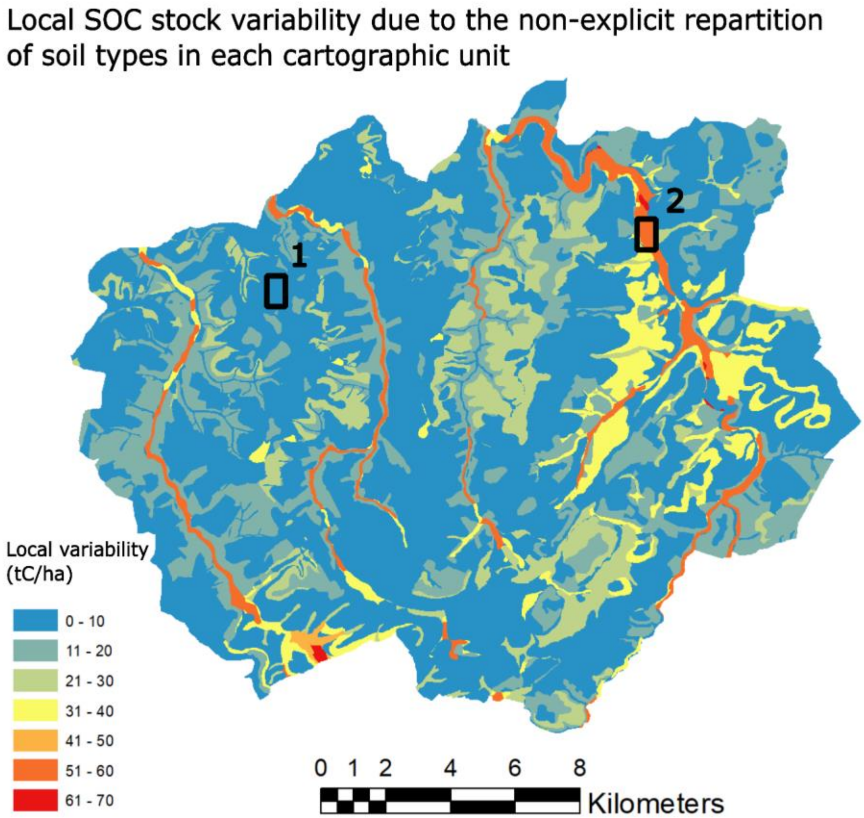


**Appendix F: Local uncertainty of SOC linked to the non-explicit repartition of soil types within the cartographic units. As an example, in zone 1, which is under forest, the represented soil types are 80% Eutric cambisol (157 tC ha$^{-1}$) and 20% Stagnosol (172 tC ha$^{-1}$). In zone 2, which is under grassland, the represented soil types are 80% Stagnosol (161 tC ha$^{-1}$) and 20% Gleysol (333 tC ha$^{-1}$). For this reason, the local variability of SOC stocks is higher in zone 2 than zone 1.**

**Appendix G~~Table 5~~: SOC stocks and maximum storage capacity above and ~~under~~ below 30 cm (~~under~~ below 30 cm represented in bold)**

| | | | | | | | | |
|---|---|---|---|---|---|---|---|---|
| | ~~**Median SOC stocks in 2018 (tC ha$^{-1}$)**~~ | | | | | | | |
| | ~~Cropland~~ **Median SOC stocks in 2018 (tC ha$^{-1}$)** ~~Grassland~~ ~~Forest~~ | | | **Theoretical maximum SOC stocks (75th percentile)** | **Theoretical maximum SOC stocks** ~~**All land uses**~~ **(88th percentile)** | ~~Cropland~~ **Maximum SOC accrual (tC ha$^{-1}$)** ~~Grassland~~ ~~Forest~~ | | |
| | Cropland | Grassland | Forest | All land uses | All land uses | Cropland | Grassland | Forest |
| Calcaric Rendzic Leptosol | 70<br>**8** | 155<br>**12**~~**95**~~<br>~~**6**~~ | 138<br>**11** | 155<br>**12** | ~~155~~170<br>**13**~~**2**~~ | 85<br>**5** | 60<br>**6** | 17<br>**2** |
| Calcaric Cambisol | 81<br>**19** | 155<br>**36**~~**114**~~<br>~~**20**~~ | 123<br>**24** | 155<br>**36** | 180~~55~~<br>**42**~~**36**~~ | 75<br>**17** | 41<br>**16** | 32<br>**12** |
| Hypereutric Epileptic Cambisol | 78<br>**14** | 112<br>**17** | 97<br>**10** | 112<br>**17** | 122~~12~~<br>**18**~~**7**~~ | 34<br>**3** | | 15<br>**7** |
| Hypereutric Cambisol | 63<br>**40** | 142<br>**86**~~**113**~~<br>~~**54**~~ | 104<br>**56** | 142<br>**86** | 180~~42~~<br>**109**~~**86**~~ | 78<br>**46** | 28<br>**32** | 38<br>**30** |
| Eutric Cambisol | 59<br>**43** | 130<br>**64**~~**71**~~<br>~~**19**~~ | 119<br>**38** | 130<br>**64** | 146~~30~~<br>**72**~~**64**~~ | 71<br>**22** | 59<br>**45** | 11<br>**27** |
| Dystric Cambisol | | 101<br>**68** | 76<br>**44** | 101<br>**68** | 117~~01~~<br>**79**~~**68**~~ | | | 25<br>**24** |
| Stagnosol | 64<br>**101** | 142<br>**143**~~**92**~~<br>~~**69**~~ | 76<br>**44** | 142<br>**143** | 180~~42~~<br>**182**~~**43**~~ | 76<br>**42** | 50<br>**74** | 28<br>**85** |
| Gleysol | 78<br>**202** | 187<br>**289**~~**156**~~<br>~~**177**~~ | 114<br>**58** | 187<br>**289** | 209~~187~~<br>**324**~~**289**~~ | 110<br>**87** | 32<br>**111** | |

**Mis en forme :** Anglais (Royaume-Uni)
**Tableau mis en forme**
**Mis en forme :** Anglais (Royaume-Uni)
**Mis en forme :** Anglais (Royaume-Uni)
**Mis en forme :** Police :Gras, Anglais (Royaume-Uni)
**Mis en forme :** Anglais (Royaume-Uni)
**Mis en forme :** Police :Gras, Anglais (Royaume-Uni)
**Mis en forme :** Police :Gras, Anglais (Royaume-Uni)
**Mis en forme :** Police :Gras, Anglais (Royaume-Uni)
**Mis en forme :** Police :Gras
**Mis en forme :** Anglais (Royaume-Uni)
**Mis en forme :** Police :Gras
**Mis en forme :** Anglais (Royaume-Uni)
**Mis en forme :** Police :Gras, Anglais (Royaume-Uni)
**Mis en forme :** Anglais (Royaume-Uni)
**Mis en forme :** Police :Gras, Anglais (Royaume-Uni)
**Mis en forme :** Anglais (Royaume-Uni)
**Mis en forme :** Police :Gras
**Mis en forme :** Anglais (Royaume-Uni)
**Mis en forme :** Normal
**Mis en forme :** Normal
**Mis en forme :** Normal

775

| Years | Calcaric rendzic leptosol | | | Calcaric cambisol | | | Hypereutric epileptic cambisol | | Hypereutric cambisol | | | Eutric cambisol | | | Dystric Cambisol | Stagnosol | | | Gleysol | |
|---|---|---|---|---|---|---|---|---|---|---|---|---|---|---|---|---|---|---|---|---|
| | C | G | F | C | G | F | C | F | C | G | F | C | G | F | F | C | G | F | C | G |
| 1 | 1.5 | 1.0 | 0.5 | 1.5 | 1.0 | 0.5 | 1.5 | 0.5 | 1.5 | 1.0 | 0.5 | 1.5 | 1.0 | 0.5 | 0.5 | 1.5 | 1.0 | 0.5 | 1.5 | 1.1 |
| 10 | 12.6 | 8.6 | 4.6 | 12.5 | 8.6 | 4.6 | 12.9 | 4.6 | 12.6 | 8.7 | 4.5 | 13.1 | 8.8 | 4.6 | 4.6 | 12.8 | 8.8 | 4.6 | 12.3 | 8.9 |
| **25** | **23.7** | **16.2** | **8.7** | **22.9** | **15.8** | **8.4** | **24.5** | **8.6** | **23.7** | **16.2** | **8.5** | **26.0** | **17.3** | **9.1** | **9.4** | **23.6** | **16.4** | **8.7** | **21.3** | **15.5** |
| 50 | 32.6 | 22.2 | 11.9 | 30.6 | 21.0 | 11.2 | 34.3 | 11.9 | 32.2 | 21.9 | 11.5 | 37.5 | 24.8 | 13.0 | 14.4 | 33.1 | 23.1 | 12.2 | 27.6 | 20.1 |
| 100 | 39.1 | 26.3 | 14.0 | 36.0 | 24.4 | 13.0 | 40.9 | 14.0 | 38.2 | 25.7 | 13.5 | 46.5 | 30.3 | 15.9 | 18.8 | 40.6 | 27.9 | 14.6 | 32.7 | 23.3 |
| 200 | 45.5 | 30.0 | 16.0 | 41.8 | 27.8 | 14.9 | 46.7 | 15.7 | 44.2 | 29.4 | 15.4 | 54.0 | 34.5 | 18.0 | 22.1 | 49.1 | 32.7 | 16.8 | 40.1 | 27.6 |
| 5000 | 84.5 | 52.1 | 27.4 | 78.9 | 48.4 | 26.4 | 92.4 | 27.6 | 98.5 | 60.1 | 32.1 | 133.8 | 69.6 | 36.2 | 50.0 | 142.3 | 77.9 | 36.1 | 118.5 | 64.1 |
| | SOC accrual after 25 years under temperature increase of 1.0 °C by 2050 (RCP 4.5 scenario) | | | | | | | | | | | | | | | | | | | |
| **25** | **21.5** | **13.6** | **5.5** | **20.2** | **12.5** | **5.3** | **22.1** | **6.2** | **21.4** | **13.0** | **5.8** | **24.1** | **15.5** | **6.5** | **8.0** | **21.3** | **13.8** | **5.9** | **17.8** | **10.5** |
| | SOC accrual after 25 years under temperature increase of 1.3 °C by 2050 (RCP 8.5 scenario) | | | | | | | | | | | | | | | | | | | |
| 25 | 20.8 | 12.9 | 4.5 | 19.4 | 11.4 | 4.3 | 21.4 | 5.5 | 20.7 | 12.1 | 5.0 | 23.5 | 14.9 | 5.8 | 7.5 | 20.5 | 13.0 | 5.1 | 16.7 | 9.0 |

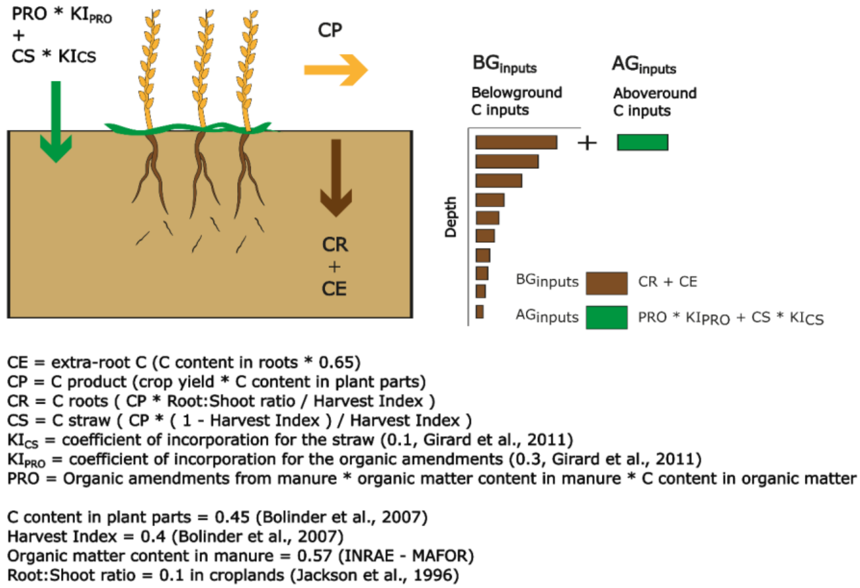


**Appendix IFigure 3: SOC stocks and maximum SOC additional storage capacity, with lower and upper confidence intervals as estimated by the bootstrap method. The SOC stock in the region of study ranges from 2.4 – 5.3 MtC and the maximum SOC additional storage capacity 1.2 - 4.1 MtC.**

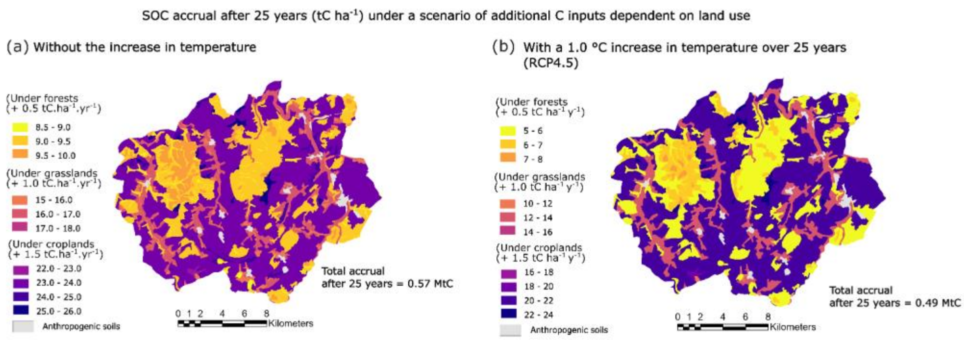


**Appendix JFigure 4: SOC accrual after 25 years under a scenario of additional C inputs dependent on land use, (a) with temperatures staying at their 2018 level, and (b) with a 1.0 °C increase in temperature over 25 years, increasing the C mineralization rates according to the correction factors of the AMG model. The attenuation in SOC accrual due to increased mineralization rates is (0.49 – 0.57) / 0.57 = 14%. The 1.0 °C increase in temperature was obtained from model simulations of mean annual temperatures by the Meteo France ALADIN63_CNRM-CM5 model under scenario RCP4.5, within an 8 km radius area around Bure (55087), comparing the year intervals 2046-2055 and 2009-2019. Source: Drias, données Météo-France, CERFACS, IPSL.**

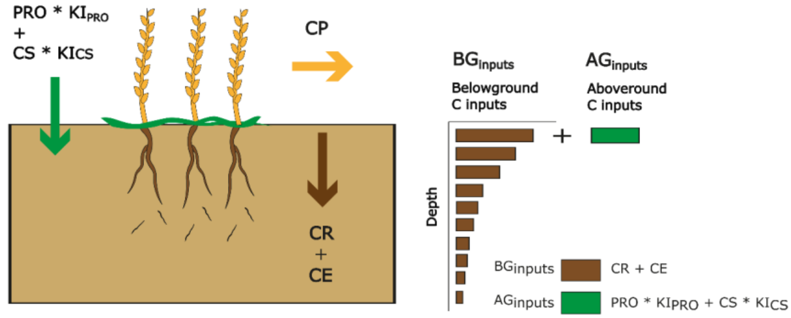


CE = extra-root C (C content in roots * 0.65)
CP = C product (crop yield * C content in plant parts)
CR = C roots ( CP * Root:Shoot ratio / Harvest Index )
CS = C straw ( CP * ( 1 - Harvest Index ) / Harvest Index )
$KI_{CS}$ = coefficient of incorporation for the straw (0.1, Girard et al., 2011)
$KI_{PRO}$ = coefficient of incorporation for the organic amendments (0.3, Girard et al., 2011)
PRO = Organic amendments from manure * organic matter content in manure * C content in organic matter

C content in plant parts = 0.45 (Bolinder et al., 2007)
Harvest Index = 0.4 (Bolinder et al., 2007)
Organic matter content in manure = 0.57 (INRAE - MAFOR)
Root:Shoot ratio = 0.1 in croplands (Jackson et al., 1996)

Appendix ~~Figure~~ K~~1~~: Estimation of the current incorporated C inputs in croplands via a yield-based allocation coefficients method from Bolinder ~~et al.~~*et al.* (2017) using agricultural yield and amendment values based on compiled reports from 2010-2019 in the region of study. The allocation coefficients were derived from the literature (harvest index and carbon content in plant parts from Bolinder ~~et al.~~*et al.* (2007), organic matter content in manure from Houot ~~et al.~~*et al.* (2014), root:shoot ratios in croplands from Jackson ~~et al.~~*et al.* (1996), incorporation coefficients form Girard ~~et al.~~*et al.* (2011)). Estimated C inputs in the croplands in the region of study are 1.4tC $ha^{-1}$ $y^{-1}$, with a mean winter wheat yield value of 5.53 tDM $ha^{-1}$ $y^{-1}$ and an amendment value of 2.13 tDM $ha^{-1}$ $y^{-1}$. The average C inputs at the steady state obtained via model inversion in the croplands of the region of study, weighted by the proportion of each soil type in the cropland areas, amount to 1.7 tC $ha^{-1}$ $y^{-1}$.

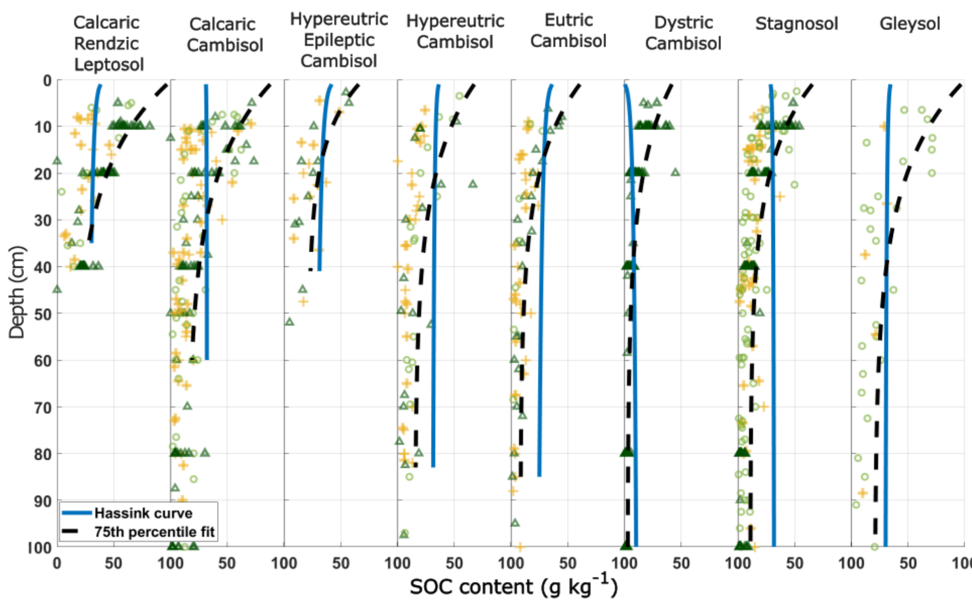


**Appendix L: Carbon saturation curves from Hassink as a function of depth. The Hassink equation was established empirically on the basis of 20 Dutch grassland soils considered to be at the stationary state, as follows: $C_{sat}$ = 4.09 +0.37 * (Clay + fineSilt) (%) where $C_{sat}$ is the theoretical carbon saturation concentration in the fine fraction in g kg$^{-1}$. The Hassink equation provides unrealistic profiles of maximum SOC content distribution in the fine fraction at depth below 30 cm, especially in the Hypereutric Cambisol, Eutric Cambisol and Stagnosol, as the equation only accounts for soil texture and does not consider the biotic controls on C inputs and SOC decomposition rates. As comparison, the 75$^{th}$ percentile fit represents a theoretical maximum SOC content in both the fine fraction and the particulate organic matter.**